THE ROLE OF PERIVASCULAR ADIPOSE TISSUE AND INFILTRATING MACROPHAGES IN VASCULAR DYSFUNCTION WITH INFLAMMATORY BOWEL DISEASE

A Thesis presented to

the Faculty of the Graduate School at the

University of Missouri-Columbia

In Partial Fulfillment

of the Requirements for the Degree Master of

Sciences

---

by

SAMUEL W. JENKINS III

Dr. Erika M. Boerman, Thesis Supervisor

DECEMBER 2022

The undersigned, appointed by the dean of the Graduate School, have examined the thesis entitled:

THE ROLE OF PERIVASCULAR ADIPOSE TISSUE AND INFILTRATING MACROPHAGES IN VASCULAR DYSFUNCTION WITH INFLAMMATORY BOWEL DISEASE

presented by Samuel W. Jenkins III,

a candidate for the degree of Master of Science,

and hereby certify that, in their opinion, it is worthy of acceptance.

Erika M. Boerman

Steve S. Segal

Timothy L. Domeier

Acknowledgements

First, I would like to express gratitude to my thesis advisor, Dr. Erika Boerman, who was instrumental in my success during this Masters program. She instilled in me a desire for excellence, integrity, and inquisitiveness in my research, while promoting a positive and learning lab atmosphere. she personified an upstanding scientist and mentor with her patient, empathetic and optimistic demeaner. So too, I would like to thank Mrs. Elizabeth Borgmann-Grunz who has been an essential part of my progression in the laboratory through her patience and willingness to teach me. I also thank the members of my master's committee, Drs. Steven Segal and Timothy Domeier, for their insightful guidance and critiques during my time in the program. I would like to thank my family. I want to express gratitude to my parents, Sean and Andrea, for their support. I want to recognize my brothers, Brian and Aidan, for always believing in me. I want to thank my partner, Aleesa for her unwavering love and understanding during my studies. Without their support, I would not be standing where I am today, and for that I am forever grateful. Finally, I would like to dedicate this master's work to my grandfather, Samuel Willis Jenkins Jr. He helped instill a love for science and drive to understand the unknown world around me.

Table of Contents

List of Tables

List of Figures

List of Abbreviations

ADCF - Adipocyte-derived relaxing factor

ADRF - Adipocyte-derived relaxing factor

AT – Adipose tissue

BAT – Brown adipose tissue

CAD – Coronary artery disease

CD68 - Cluster of Differentiation 68

CD86 - Cluster of Differentiation 86

CD163 - Cluster of Differentiation 163

CD206 - Cluster of Differentiation 206

DSS – Dextran sodium sulfate

eNOS – Endothelial nitric oxide synthase

IBD – Inflammatory bowel disease

IFN-ɣ - Interferon gamma

iNOS – Inducible nitric oxide synthase

IL - Interleukin

LPS - Lipopolysaccharide

LFA-1 - Lymphocyte function-associated antigen 1

MA – Mesenteric artery

MCP-1 – Monocyte chemoattractant protein 1

NADPH - Nicotinamide adenine dinucleotide phosphate

NO – Nitric oxide

PVAT - Perivascular adipose tissue

TGF-β – Tumor growth factor – beta

Th – T-helper

Th1 – Type 1 T-helper response

Th2 – Type 2 T-helper response

TLR – Toll like receptor

TLR-4 – Toll-like receptor 4

TNF- α - Tumor necrosis factor alpha

UCP1 - uncoupling protein 1

VSMC – Vascular smooth muscle cell

WAT – White adipose tissue

Introduction

Adipose Tissue

Historically, adipose tissue (AT) throughout the body has been categorized as either brown adipose tissue (BAT) or white adipose tissue (WAT). These categories are determined by color, physical characteristics, and physiological functions of the adipocytes of the tissue. WAT is the predominant subtype found in humans with two major depot types: subcutaneous WAT under the skin and visceral WAT, which surrounds the internal organs (Richard et al., 2000). Subcutaneous WAT is located under the skin and acts as a protective barrier against infections, an insulator of body heat and protection against external mechanical stress. The adipocytes in WAT are generally a sphere-shaped cell (Richard et al., 2000; Trayhurn & Beattie, 2001). Because of the single large lipid droplet within the cell, the normal cell organelles are pushed to the cell's periphery. White adipose tissue has a large capacity for lipid storage, thus contributing to its dysfunctional involvement in obesity and dyslipidemia. Further, its structural plasticity allows rapid changes in adipocyte size and/or number (i.e., hypertrophy vs hyperplasia) based on global and local metabolic conditions (Sakers et al., 2022). Regardless of location, WAT was originally thought to function only in energy homeostasis, by taking up excess lipids and store them as triglycerides or breaking them down and releasing the lipids as fatty acids via *de novo* lipogenesis (Richard et al., 2000; Trayhurn & Beattie, 2001). However, the discovery of leptin in 1990 quickly changed this limited thinking (Zhang et al., 1994). Continued discovery of even more adipose-derived factors, or adipokines, highlighted WAT as a dynamic endocrine tissue that plays an active role in both health and disease. Adipokines include hormones, pro- and anti-inflammatory cytokines, and other proteins

with a ride range of global and tissue-specific effects. Overall, adipose research now shows that WAT is involved in inflammation, metabolism and endocrine/paracrine signaling.

Brown adipose tissue (BAT) functions as a thermal regulator via non-shivering thermogenesis (Cannon & Nedergaard, 2004). As a specialized AT, BAT represents a relatively small proportion of total adipose and functions as a thermal regulator via non-shivering thermogenesis. There are six anatomic regions that are considered activated BAT depots —cervical, supraclavicular, axillary, mediastinal, paraspinal, and abdominal— with a majority of all activated BAT concentrated in a continuous layer within the upper torso (Leitner et al., 2017). A specialized, BAT-specific protein called uncoupling protein 1 (UCP1) mediates the uncoupling of mitochondrial respiration necessary for this thermogenesis (Richard et al., 2000). This allows for heat generated by the BAT to dissipate. Brown adipose also contains lipid droplets, but they are smaller than those in WAT and dispersed throughout the cell along with an increased number of iron-containing mitochondria in comparison to white adipose, which gives the tissue its brownish hue (Cannon & Nedergaard, 2004). BAT is found in large quantities in mammals postnatally and during hibernation. In humans, it was initially thought that brown adipose was only present in infants, however it has been found that adult humans have BAT depots with changes to BAT activity occurring during times of external environmental change (Richard et al., 2000).

Recently, another phenotype of adipose has been described. Beige adipose tissue shares similar characteristics and function to both brown and white adipocytes. They are thought to develop from a subpopulation of preadipocytes or from the “browning” of WAT into a “browner” phenotype, caused by the high iron-containing mitochondria. The result

is an adipocyte with large lipid droplets, increased mitochondria, and protection against metabolic dysfunction in comparison to WAT adipocytes (Cannon & Nedergaard, 2004). The beige phenotype is relatively unstable, and beige adipocytes often re-whiten, becoming indistinguishable from WAT that never underwent the browning process (Mulya & Kirwan, 2016).

Perivascular Adipose Tissue

PVAT in Health

Perivascular adipose tissue (PVAT) is a unique fat depot representing ~3% of adipose tissue that surrounds the blood vessels with both local and systemic effects (Siegel-Axel & Häring, 2016). Importantly, there are functional and phenotypic differences that exist in PVAT depots that differentiate PVAT from other adipose tissues. The specific vascular bed region often determines the differences seen in PVAT function and phenotype. PVAT can be WAT-like, BAT-like or mixed, depending on the region of the vascular bed. BAT is generally limited to the thoracic aorta, whereas the resistance vasculature is generally surrounded by WAT. The presence of mixed/beige adipose appears depends largely on physiological or experimental conditions, but it is most commonly found surrounding the abdominal aorta and kidneys (Brown et al., 2014). Each of these phenotypes may have different levels of vascularization, innervation and adipokine profiles that elicit region-specific responses. The lineage differences in PVAT tissues are highlighted in murine models with smooth muscle (SM22α)-specific PPAR-gamma deletion. While these mice lack PVAT in the abdominal aorta and mesenteric regions, BAT and some other non-PVAT WAT such as subcutaneous and visceral adipose remain intact (Xiong et al., 2018). This alludes to PVAT being a heterogeneous and specialized adipose tissue with inherent differences in developmental and secretory properties compared to adipocytes from other fat depots. The PVAT around mesenteric resistance arteries, which is the focus of the current study, is composed exclusively of WAT. Consistent with WAT, it has low mitochondrial content, low expression of UCP-1 and relatively large single lipid droplets. Its reported absence in the SM22α-PPAR gamma knockout mice suggests that it

shares important developmental origins with nearby vascular smooth muscle, but the overall field of PVAT origin remains mostly undefined (Chatterjee et al., 2009).

Most blood vessels outside of the brain and lungs are surrounded by varying amounts of PVAT. PVAT lies outside of the vascular adventitia, but still interacts physically and functionally with the underlying layers of the vasculature. Blood vessels are comprised of three layers: tunica adventitia, tunica media and tunica intima with the PVAT surrounding the external-most layer; the tunica adventitia. In the resistance vasculature, PVAT exists in a fairly seamless continuum with the adventitia. Because our study centers on mesenteric PVAT, this will be the primary focus of further PVAT discussion. Structurally, healthy PVAT contains ~70% adipocytes. The remainder is comprised of the stromal vascular fraction, which includes nerves, immune cells, vascular cells, and stem cells (Szasz et al., 2013). Mesenteric PVAT is heavily and continuously innervated, with both sensory and sympathetic nerves playing a role in its vascular and non-vascular functions (Westcott & Segal, 2013). Vascular cells are present due to the microcirculation within the PVAT. Immune cells of all types are interspersed throughout PVAT, and their functions vary by both cell type and physiological state.

Until recently, PVAT was seen primarily as a mechanical modulator of vessel function. However, now it has been recognized as a major player in vascular homeostasis via modulation of both smooth muscle and endothelial function. In the healthy mesenteric vasculature, the presence of PVAT has a collectively anticontractile effect, meaning its presence and net physiological function decreases the level of constriction of mesenteric arteries (Soltis & Cassis, 1991). Many signaling mechanisms contribute to this effect, and they remain incompletely defined. The overall anticontractile effect is linked to one or

more releasable vasoactive substances commonly referred to as Adipocyte-derived relaxing factor (ADRF). Key candidates for ADRF include adiponectin, hydrogen peroxide, hydrogen sulfide, prostacyclin, and angiotensin 1-7 (Szasz et al., 2013), but it has not been conclusively identified and may include multiple or variable components. Adipokines are generally considered the most important category of releasable factors because of their adipose tissue origin and cytokine-like effects. It should also be noted that some adipokines are also produced by the immune cells of the PVAT, not only by the adipocytes. These adipokines can modulate several physiological functions and can be categorized to having a vasorelaxant effect, a vasoconstrictive effect, or both. Some examples of vasodilatory adipokines include adiponectin, omentin, and visfatin. PVAT can also induce pro-contractile effects on VSMCs with the release of adipocyte-derived constricting factors (ADCF). The release of ADCFs promotes vasoconstriction of the smooth muscles and an overall vasoconstriction the artery (Chang et al., 2020; Richard et al., 2000). Vasoconstrictive adipokines include nesfatin, resistin, chemerin and angiotensin II. Many adipokines have mixed vascular effects depending on their concentration and other physiological conditions. These include leptin, tumor necrosis factor, interleukin-6, apelin and various reactive oxygen species (Cheng et al., 2018). These factors are released by the PVAT and reach the medial and endothelial layers of the blood vessels via direct diffusion or the vasa vasorum in larger arteries (Xia & Li, 2017). It is important to note that like many other physiological processes, adipokines and the other factors secreted by PVAT must collectively create a balance between vasoconstrictive and vasodilatory effects for healthy vascular homeostasis. When disequilibrium in this process occurs, disease states begin to develop.

Adipokines can also be categorized as pro- and anti-inflammatory (Cheng et al., 2018; Richard et al., 2000). This relates to the response they produce in inflammatory signaling of the immune system. Surrounding and between the densely packed adipocytes are the resident immune cells of stromal vascular fraction: fibroblasts, CD4 & CD8 T cells, mast cells, natural killer cells, B cells, macrophages, and neutrophils (Cheng et al., 2018; Szasz & Webb, 2012). The release of pro-inflammatory adipokines can cause the activation of resident immune cells in addition to proliferation and recruitment of pro-inflammatory immune cells and infiltration of other immune cells in response to downstream signals elicited by the pro-inflammatory factors. The release of anti-inflammatory factors causes de-activation of certain immune cells and recruitment and proliferation of anti-inflammatory immune cells. Under physiological conditions, PVAT secretes mainly anti-inflammatory adipokines such as adiponectin, nitric oxide (NO), and omentin.

PVAT in Disease

Because of PVAT's important role in promoting normal blood flow and controlling blood pressure, changes in its composition and function are linked to multiple disease states. Most of what is currently known about PVAT function in disease comes from studies of atherosclerosis, obesity, and hypertension. Studies of obesity and hypertension are of interest to the current work because they affect the mesenteric resistance arteries that are used for our studies. Obesity has numerous adverse effects on cardiovascular structure and function and is associated with increased risk for cardiovascular disease and remodeling of adipose tissue (Csige et al., 2018). Obese patients are more likely to develop hypertension and have a higher risk of stroke (Akil & Ahmad, 2011). Increased abdominal adiposity is a key feature of obesity. Because mesenteric PVAT is also comprised of WAT, it is similarly susceptible to hypertrophy and hyperplasia, which are key indicators of

metabolic disease (Bussey et al., 2016). In humans, the amount of PVAT surrounding the aorta is increased with obesity, but the extent of mesenteric PVAT expansion has not been accurately quantified. The increase in aortic PVAT mass correlates with hypertension, diabetes, and aortic/coronary calcification, even when corrected for body-mass index. Obesity also has drastic effects on the stromal vascular fraction of PVAT (Szasz et al., 2013). The total number of macrophages, T and B cells, neutrophils, dendritic cells and mast cells have all been shown to increase in PVAT with obesity. Only eosinophils are known to decrease within PVAT in disease pathogenesis. Macrophages make up the greatest proportion of stromal vascular fraction in health, and their numbers appear to increase to the greatest extent in both obesity and hypertension (Saxton et al., 2019; Weisberg et al., 2003).

In addition to structural changes, obesity is associated with significant changes in the function of PVAT with respect to the underlying arteries. In obese individuals, PVAT goes through physiological changes, going from an anti-contractile, vasodilatory effect to a pro-contractile vasoconstrictive state (Xia & Li, 2017). The production of vasodilatory adipokines by PVAT, including hydrogen sulfide, adiponectin and NO are reduced in obese individuals. The healthy anti-contractile effect of PVAT is completely lost in mouse models of diet-induced obesity and genetic models of metabolic syndrome. The underlying mechanism for this PVAT dysfunction is not clearly defined but linked to the "obesity triad". This consists of PVAT hypoxia, inflammation, and oxidative stress that leads to a pro-inflammatory profile of PVAT-derived adipokines. Obesity causes unhealthy expansion of adipose tissue, including PVAT. Global expansion of WAT in obesity results in elevated basal lipolytic rate. This enhances the release of fatty acids which, when

compounded by the now abundant pro-inflammatory adipokines and chemokines, contributes to the development of insulin resistance and inflammation. Adipocyte hypertrophy in conjunction with capillary rarefaction and angiogenesis promotes cellular hypoxia in PVAT. Hypoxia stimulates the release of inflammatory cytokines and chemokines from PVAT adipocytes and infiltrating macrophages (Cheng et al., 2018). It is thought that the infiltration of macrophages is in response to PVAT inflammation, meaning macrophage inflammation occurs after the activation of PVAT inflammatory response. Macrophages then potentiate the PVAT inflammatory response and enhance the activity of nicotinamide adenine dinucleotide phosphate (NADPH) oxidase (Xia & Li, 2017). NAPDH oxidase is a major source of superoxide anions in the vasculature. Mechanistically, expression of the NADPH oxidase subunits p67phox (Ketonen et al., 2010) and Nox2 (Xia et al., 2016) is increased in the aortic PVAT of obese mice. The increased superoxide anions result in oxidative stress that enhances the overall inflammatory profile of the PVAT and macrophages, leading to a vicious cycle furthering vascular dysfunction. This cycle is further exacerbated by an imbalance in the adipokine profiles secreted by PVAT towards a more pro-inflammatory, pro-contractile state.

Adipose macrophages are key contributors to PVAT and vascular inflammation in obesity. Macrophages typically represent about 10-15% of the stromal vascular fraction of PVAT, however this drastically increases to 45-50% during obesity (Wynn et al., 2013). Since obesity is characterized by low-grade chronic inflammation and excess WAT, macrophages and adipose tissue are both major players in obesity and obesity-related diseases. Type II diabetes occurring alongside obesity is also strongly linked to the increased macrophage accumulation (in response to the chronic inflammation) and

dysregulation in production and secretion of adipokines and other factors secreted by the excessive AT that occurs in obesity (Zatterale et al., 2019). Importantly, macrophage secretion of pro-inflammatory cytokines increases in obesity, contributing to insulin resistance and ameliorating the pathogenesis. Important pro-inflammatory cytokines secreted by macrophages include tumor necrosis factor - alpha (TNF- α), interleukin (IL) 1β, IL-6, and IL-17 (Arango Duque & Descoteaux, 2014).

Changes in PVAT function are also well-documented in the pathophysiology of atherosclerosis. While atherosclerosis studies generally focus on the aorta, PVAT function here is of interest to our studies because of its clear link to immune dysfunction and inflammation. Inflammation in PVAT is highly related to atherosclerosis development (Qi et al., 2018). The pathogenesis of atherosclerosis includes endothelial dysfunction, inflammatory cell recruitment, VSMC proliferation and migration. During pathogenesis, cytokines are released by virtually all the cells in PVAT, which exert multiple effects on the surrounding tissue. It is hypothesized that PVAT plays a crucial role in the pathogenic processes of atherosclerosis, given the anatomical proximity of PVAT to the vascular wall. Interestingly, in humans, the most atherosclerotic-prone area is the coronary arteries and aorta which have an abundant amount of PVAT surrounding them. In mice, however, there is little PVAT surrounding the coronaries and mouse coronaries are highly resistant to atherosclerosis. This evidence suggests that the presence of PVAT may be associated with atherosclerosis development. Shear stress-induced endothelial dysfunction is sometimes considered the initial step in atherosclerosis development. Endothelial dysfunction is characterized by reduced bioavailability of nitric oxide. NO is produced by endothelial NO synthase (eNOS) and PVAT, and loss of this PVAT-derived NO may be an important

contributor to vascular dysfunction in atherosclerosis and other cardiovascular diseases. eNOS has many anti-atherogenic properties that allow for control of vascular smooth muscle proliferation and inhibition of platelet aggregation, leukocyte adhesion and vascular inflammation. In studies where PVAT was removed from small arteries, basal NO production was reduced, suggesting PVAT contributes to vascular NO production (Virdis et al., 2015). Obesity-induced hypertension and endothelial dysfunction in C57BL/6 mice are caused by increased expression of inflammatory cytokines and increased oxidative stress in PVAT (Ketonen et al., 2010). Adhesions of circulating inflammatory cells to the dysfunctional endothelium trigger accumulation of cholesterol to the wall of the artery (Bergheanu et al., 2017). This initiates the formation of fatty streaks and lesions where cholesterol accumulation can take place. Foam cells are recruited into the intimal layer, evolving the fatty streaks and lesions into a fibrous plaque. Eventually, the plaque can become unstable and rupture, resulting in a thrombotic occlusion of the artery.

Immune cell expansion in PVAT is now considered a critical factor in atherosclerosis pathogenesis and severity (Qi et al., 2018). Macrophages in particular play a crucial role in the pathophysiology of atherosclerosis. In mouse models, macrophage numbers increase up to 20-fold within the aortic wall during atherogenesis (Gravina et al., 2018; Moore et al., 2013). This is from circulating monocytes that later differentiate or by proliferation by the resident macrophages discussed before. They worsen the pathogenesis of the disease by amplifying the immune response with the release of pro-inflammatory cytokines and reacting with excess cholesterol and forming foam cells. These foam cells are necessary for plaque formation. Foam cell buildup and cellular debris heavily contribute to plaque growth and continued chronic inflammatory response. Additionally,

macrophages have paracrine functions over VSMCs, further aiding the overall inflammatory state and signaling to produce additional pro-inflammatory cytokines and components of the extracellular matrix, which advances plaque formation and promotes trapping of lipoproteins (Barrett, 2020). Furthermore, persistent inflammation without resolution will push for macrophage apoptosis, leading to accumulation of cellular debris which will aid the necrotic core formation of the atheroma. Highlighting the importance of PVAT macrophage expansion, recent studies showed that macrophage infiltration into PVAT precedes loss of endothelial eNOS function and plaque formation in disease progression (Skiba et al., 2017). However, it is important to note that macrophages play a pivotal role in vascular homeostasis beyond atherosclerosis.

Macrophages

Macrophages are a key component of the innate defense against pathogens that partake in the inflammatory response and maintenance of tissues. They are derived from bone marrow as monocytes or develop from leukocyte precursors without a monocyte intermediate. As the sentries of the innate immune system, macrophages take residence in almost every tissue. This includes blood vessels and some of their layers, including PVAT. Even though immune cell recruitment via chemotaxis is substantial during perivascular inflammation, some immune cells are resident within the vessel wall and PVAT in health. These resident immune cells are primarily macrophages (Nosalski & Guzik, 2017; Zhang et al., 2021). Macrophages' function and phenotype differ depending on the tissue microenvironment. Resident macrophages are essential for driving the immune response necessary for its tissue microenvironment (Davies et al., 2013; Epelman et al., 2014).

More recently, macrophages have been introduced as regulators of vascular

function. Specifically, macrophages are heavily involved in functional processes during tissue injury, repair, and regeneration (Röszer, 2018). However, dysfunction in macrophage activation is linked to various metabolic, inflammatory, and immune disorders. The functions of macrophages in tissue and vessel repair include elimination of invading pathogens and necrotic cellular waste via phagocytosis, promoting angiogenesis by guiding the sprouting of new blood vessels and stimulating the proliferation of endothelial and VSMCs, release of matrix metalloproteinase for matrix remodeling, and the secretion of pro-inflammatory cytokines and chemokines to maintain leukocytes infiltration in response to inflammation (Zhang et al., 2021). Overproduction and secretion of pro-inflammatory cytokines and chemokines by pro-inflammatory macrophages increases immune cell recruitment. Chronic immune response will result from this accumulation of immune cells and secretion of pro-inflammatory cytokines and chemokines. This process will increase oxidative stress, which will stimulate further tissue damage and promote endothelial dysfunction.

Another important characteristic of macrophages to discuss is macrophage polarization. This is when tissue macrophages undergo rapid in situ phenotype change in response to signaling factors (Röszer, 2018). Macrophage polarization occurs via different activation pathways necessary for them to carry out the defensive function. Macrophages can modify their physiologic function via polarization from unpolarized to either an anti-inflammatory, healing/growth promoting state known as M2 (alternative activation) or a pro-inflammatory, killing/inhibitory state known as M1 (classical activation) (Murray, 2017). The M1/M2 classification system was first introduced in 2000 and generally refers to the M1 and M2 macrophage propensity to stimulate T-helper (Th) types 1 and 2 (Th1

and Th2) cytokine responses, respectively, in mice (Mills et al., 2000). *In vitro*, M1 macrophages are typically generated with exposure to lipopolysaccharide (LPS) and interferon gamma (IFN-ɣ) or TNFα. These cultured M1 cells then release increased amounts of the proinflammatory mediators IL-1β, TNFα, IL-6, IL-12, inducible nitric oxide synthase, and others. In contrast M2 macrophages are typically induced with IL-4, (most common) and IL-13 and secrete a wide array of including anti-inflammatory mediators IL-10 and transforming growth factor beta (TGF-β) (Murray, 2017). Because of the more complex activation and release profiles of M2 macrophages, subtypes have been proposed to differentiate M2a, M2b and M2c populations. However, there is still a large degree of disagreement on these classifications between studies (Shapouri-Moghaddam et al., 2018). Both M1 and M2 macrophages are associated with expression of specific cell surface markers that are often used experimentally to separate each phenotype. In mice, the most commonly used cell-surface M1 markers are CD86, CD68 and iNOS. M2 classification is complicated by subtype differences, but the most common surface markers used experimentally are CD206 and CD163 (Scientific, 2021).

Classifying macrophage populations *in vivo* is much more complex and controversial due to the enormous variation in local activating signals and cytokine release profiles. Due to new technologies like advanced flow cytometry and single cell RNA sequencing, it is now clear that M1 and M2 macrophages exist in a spectrum, rather than defined phenotypes (Xue et al., 2014). For example, macrophages in transition may express markers and secrete cytokines associated with both M1 and M2 macrophages, either temporarily or permanently depending on physiological/experimental conditions. Recent in-depth studies comparing *in vitro* and *in vivo* macrophage populations after exposure to

typical *in vitro* activators show that there is surprisingly little correlation between macrophage activation *in vivo* and M1/M2 polarization *in vitro* (Orecchioni et al., 2019). The authors indicate that much more work is needed to discover and validate M1 and M2 markers *in vivo*.

Persistent and chronic shifts towards the M1 phenotype are associated with many inflammation-driven disorders. For instance, in obesity, resident and infiltrating macrophages found in adipose tissue shift towards the M1 phenotype. Toll-like receptors (TLR) and inflammasomes responsible for macrophage proliferation are activated in obesity, priming the macrophages for contribution to the low-grade chronic inflammation. An important TLR is TLR-4, which has increased expression on adipose tissue macrophages. TLR-4 deficient mice fed a high fat diet improves AT inflammation, insulin resistance and adiposity. A shift towards M2 adipose tissue macrophages is associated with lean AT and insulin sensitivity (Castoldi et al., 2015). In atherosclerosis, M1-like macrophages are associated with symptomatic plaques that lack structural integrity, meaning they have the possibility of rupturing and developing into a thrombus. In general, M1-like macrophages promote the inflammatory pathway. M1 macrophages are associated with macrophage apoptosis and/or necrosis, leading to build up of cellular debris that contributes to the necrotic core (de Gaetano et al., 2016). The necrotic core growth correlates with increased instability and vulnerability of the plaque to rupture. In contrast, M2-like macrophages are abundant with asymptomatic, stable plaques (Bi et al., 2019). They play a balancing act with their counterparts, attempting to ameliorate the pro-inflammatory effects of the M1 by preventing necrotic buildup and clearing cellular debris in hopes of resolving the inflammation. This is known as efferocytosis and when it is not

sufficient, M1 macrophages will begin to form the necrotic core.

There is ongoing debate as to whether macrophages involved in vascular dysfunction are predominantly resident or infiltrating, and most of what is known in PVAT is assumed based on studies in the vascular adventitia Many resident macrophages in the vasculature are largely yolk-sack derived and exist at birth, while others are populated after birth from the bone marrow (Ensan et al., 2016). These existing macrophages are important because in response to injury or inflammation, they can proliferate and secrete chemotactic signals like macrophage chemoattractant protein 1 (MCP-1) that recruit additional macrophages to the PVAT and adventitia (Nosalski & Guzik, 2017). The balance of resident vs recruited macrophages in PVAT and adventitia is largely a debate of "outside-in" or "inside-out" movement of macrophages during the inflammatory response associated with macrophage proliferation (Abram & Lowell, 2009). An "inside-out" response is characterized by leukocyte extravasation where leukocytes, in this case monocytes, adhere to the walls of the vessel and pass through the endothelium due to impaired barrier permeability from the chronic inflammation (Abram & Lowell, 2009). So, the description of "inside-out" pertains to the leukocyte originating from the "inside" of the vessel (the lumen) before adhering to the vessel wall and extravasating "outwards" into the layers of the vessel itself. Once these macrophages are activated, they will secrete pro-inflammatory cytokines that will promote ROS production and further vascular dysfunction. An "outside-in" response is often attributed to the activation and proliferation of resident leukocytes within the adventitia and PVAT itself that then affects inner vascular layers (Maiellaro & Taylor, 2007). However, it can also involve recruitment of immune cells from outside the PVAT, as a variety of vascular injuries can lead to rapid influx of

leukocytes into the adventitia (Okamoto et al., 2001). In addition to an array of well-defined chemokines and chemokine receptors, a main activator that is often discussed in the case of "outside-in" inflammatory response is increased ROS production causing oxidative stress (Stenmark et al., 2013). Upon production of these chemotactic factors, leukocytes migrate to the vessel wall and proliferate within the adventitia, resulting in an accumulation of immune cells that are secreting pro-inflammatory cytokines and factors. The cytokine and chemokine profile at this point is shifted towards a pro-inflammatory state in most diseases, with increased M1 macrophage proliferation in response to the inflamed tissue microenvironment. This migration will recruit further immune cells and continually promote further inflammatory response and additional abnormal immune response. If this inflammation response becomes chronic, such as what is exhibited during obesity-induced inflammation, immune and vascular dysfunction will compound, leading to the development of multiple pathogenic pathways. There is also evidence that macrophages, particularly in atherosclerosis, can have long-term epigenetic or metabolic reprogramming that keeps them in a more M1-like phenotype and increases the magnitude of subsequent inflammatory responses (Park, 2021).

Inflammatory Bowel Disease

Inflammatory Bowel Disease (IBD) is an umbrella term encompassing two main clinical manifestations: Crohn's disease and ulcerative colitis. As of 2015, 3.1 million US adults (1.3%) have received a diagnosis of IBD in comparison to 1.8 million (0.9%) in 1999, and the prevalence of IBD is expected to continue rising in worldwide. The etiology of IBD is complicated, with onset linked to combinations of genetic susceptibility, immune system changes, altered gut microbiome, and environmental triggers (Guan, 2019).

Lifestyle factors may also play a key role, as IBD continues to rise in prevalence in parallel with the rise in obesity and expansion of the Western diet across the world (Bilski et al., 2019). IBD is a chronic autoimmune condition characterized by chronic abnormal immune response and both intestinal and extraintestinal inflammation. Importantly, intestinal blood flow decreases, and bowel ischemia increases in IBD (Harris et al., 2010; Hultén et al., 1977; Thornton & Solomon, 2002). The mesenteric arteries are the main source of blood directly to the intestines, and therefore represent a likely site of vascular dysfunction. Consistent with vascular dysfunction in IBD, patients experience increased risk of many cardiovascular diseases including stroke, heart failure, myocardial infarction, and atherosclerosis despite having lower traditional factors (obesity, hypertension, diabetes) in comparison to the general population (Aniwan, Pardi, et al., 2018). This suggests that the underlying pathophysiology of these cardiovascular comorbidities may differ in IBD patients compared to healthy individuals.

Changes in adipose tissue have long been associated with IBD. Especially in Crohn's disease, patients consistently have an increased ratio of pathogenically altered intraabdominal fat vs abdominal fat that is commonly known as "creeping fat" (Crohn et al., 1932). Creeping fat can be distinguished from normal mesenteric fat-tissue by its larger amount, greater immune cell infiltration, and increased secretion of inflammatory mediators (Bilski et al., 2019). Little is known about the role of PVAT in IBD, as it has only recently been recognized for its active contribution towards vascular function and homeostasis. Creeping fat is known to encompass mesenteric artery branches in human IBD patients, but it is unclear whether or how this affects the existing underlying PVAT (Feng et al., 2018). One recent study suggests that PVAT protects against endothelial

dysfunction but not reactive oxygen species formation in the aorta with IBD, but much more research is needed to characterize the role of PVAT in vascular dysfunction with IBD (Wu et al., 2022).

Macrophages became an area of interest in IBD because of their important immune functions, their function as vascular regulators in the vessels of the gut, and their large populations found in the healthy intestinal mucosa. In the intestine, macrophages play a critical role in both homeostasis and disease. In healthy intestinal mucosa, $Ly6C^{hi}$ (in mice) and $CD14^{hi}$ (in human) monocytes constantly enter the intestinal mucosa and differentiating into mature $CX3CR1^{hi}$ F4/80+ macrophages. Here, they function as phagocytic agents and produce a balance of pro-and anti-inflammatory cytokines in response to antigens (Bain & Mowat, 2014). Resident macrophages in the intestine can then further differentiate in phenotype and function based on conditions in their location, but each contribute to the function of nearby blood vessels, where there is a close association with macrophages (Honda et al., 2020). The lamina propria has the largest population of macrophages, which are located close to the epithelium. These macrophages survey the environment, engulf antigens, and promote cell renewal through their cytokine profiles. Macrophages also localize near lamina propria vasculature and are critical for vascular repair. In the muscularis, macrophages near the enteric nervous system contribute to intestinal motility and secretion (Gabanyi et al., 2016). The submucosal resident macrophages are self-renewing and primarily support nearby vasculature. The serosa contains the smallest population, which also contribute to motility and tissue repair (Honda et al., 2020).

Intestinal macrophages are a key factor in the development of IBD. In the

development of inflammation, intestinal macrophage can respond to both normal self-antigens like commensal gut bacteria and to pathogenic antigens by producing a prolonged, unresolved immune response (Han et al., 2021; Na et al., 2019). This change involves a significant change in the composition of the macrophage pool, particularly in the lamina propria. Resident macrophages polarize to an inflammatory M1 phenotype, leading to the release of proinflammatory cytokines, reactive oxygen species, and chemotactic signals that recruit additional monocytes to the intestine (Wu et al., 2022). Intestinal macrophages also promote the activation of T-cells and fibroblasts that perpetuate chronic inflammation. Importantly, the infiltration of circulating monocytes and activation of resident macrophages can occur within the PVAT as well, as evidenced by studies of other diseases (Guzik et al., 2017). During IBD progression, PVAT likely goes through similar physiological change and overproduces its own pro-inflammatory signaling factors, compounding the inflammatory effects alongside the dysregulation occurring in the monocytes/macrophages. However, the immune cell composition in PVAT with IBD has never been studied.

Key Previous Studies

Our laboratory is specifically interested in how both PVAT and perivascular macrophages are involved in loss of vascular function associated with IBD. Foundational experiments completed by the Boerman laboratory have given insight to the possible mechanisms that also served as the basis of this research project. All preliminary experiments utilized an IL-$10^{-/-}$ mouse model that is gavaged with *H. hepaticus*, allowing for IBD pathogenesis to occur over 90 days. Pressure myography studies using electrical field stimulation of mesenteric arteries (MAs) demonstrated profound impairment in

dilation via perivascular sensory nerves and a complete inability of those nerves to inhibit sympathetic constriction (Norton et al., 2021). RNA sequencing of intact MAs from Control and IBD mice showed that both M1 and M2 macrophage markers were among those with the greatest IBD-related expression increase. Immunofluorescence confirmed that IBD was associated with accumulation of both M1 and M2 macrophages in the adventitia of MAs. More importantly, depleting macrophages with clodronate liposome injections restored sensory vasodilation, suggesting that they are important to vascular impairment with IBD (Grunz-Borgmann et al., 2019). Parallel studies of cannulated arteries with and without PVAT showed that PVAT loses its anticontractile function in IBD and becomes pro-contractile, contributing to sympathetic constriction (Figure 1). Clodronate reverses PVAT pro-contractility, leaving it neutral but not fully anticontractile (unpublished results, not shown), suggesting that the role of macrophages in PVAT may be different and more complicated than the adventitia.

Overall, many factors remain unclear about PVAT in IBD. In normal, healthy individuals, PVAT and its macrophages act in collaboration as a communication hub to maintain vascular homeostasis. PVAT macrophages responds to the tissue microenvironment with production and secretion of anti-inflammatory, healing/growth promoting (M2-associated) and/or pro-inflammatory, killing/inhibitory (M1-associated) adipokines, chemokines and cytokines. Normally, an equilibrium must be kept by these two populations in order to maintain vascular homeostasis. In IBD, adventitial macrophages increase in number and shift towards a pro-inflammatory phenotype, meaning they produce large quantities of pro-inflammatory adipokines, chemokines and cytokines that further push the inflammatory response. Our laboratory has been able to

show key structural and physiological changes to the MA adventitia and PVAT associated with increased presence of macrophages in IBD. Several key questions remain: First, does the size or density of PVAT adipocytes change during IBD? To answer this question, we measured the size and density of adipocytes from H&E stained PVAT sections. We hypothesized that both the size and density of MA PVAT adipocytes will decrease with IBD. The second question is more complex: How does IBD affect the PVAT macrophage population throughout the pathogenesis of IBD? To gain further insight on macrophage proliferation, we characterized the populations of M1-like vs M2-like macrophages throughout IBD pathogenesis by using a time-point study of immunolabelled PVAT, looking at 1, 5, 10, 20, 40-, 80-, 160- and 240-days post gavage. We hypothesized that IBD pathogenesis works similarly to other vascular diseases as discussed above, with an early shift toward M1-like macrophages to promote the inflammatory response. We anticipate that a later timepoint shift towards M2-like macrophage populations may associated with a plateau in inflammation. Results from this study will shed light into possible intervention points during IBD pathogenesis where treatment options may be utilized.

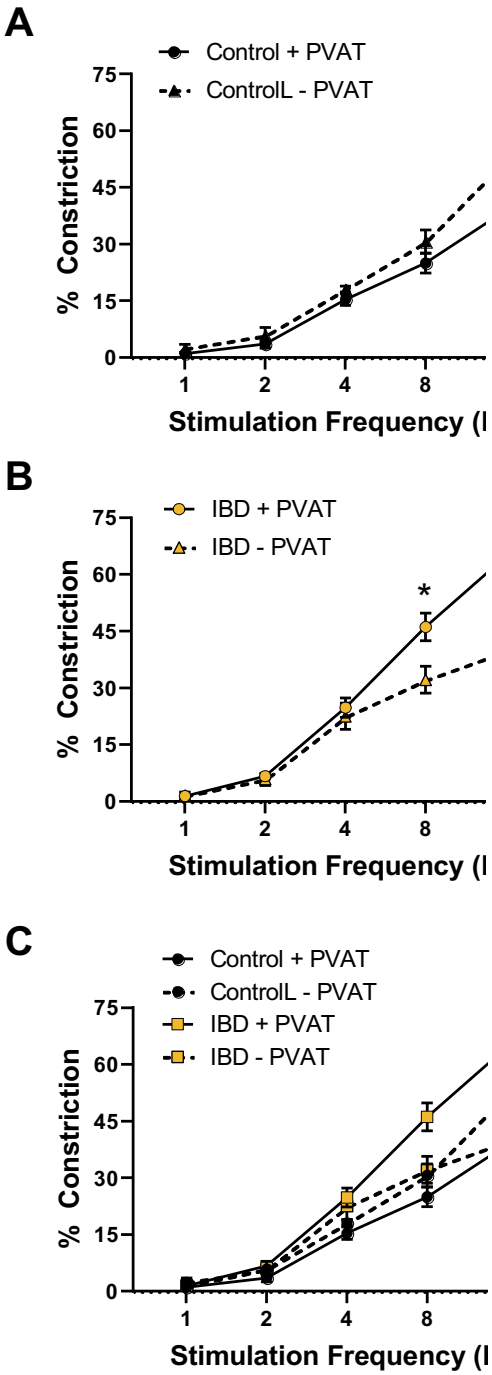

Figure 1. Mesenteric artery PVAT becomes pro-contractile with IBD. Data are mean +/- SE constrictions resulting from electrical field stimulation-induced (1-16 Hz) sympathetic constrictions of isolated, cannulated, and pressurized arteries with (solid lines) or without (dashed lines) attached PVAT in PSS from (A) Control and (B) IBD mice. For A-B *=$p<0.05$ +PVAT vs –PVAT. N=4-6 mice (vessels?) per group. C shows the data from A and B graphed together, highlighting a main effect of PVAT that is anticontractile in Control and pro-contractile in IBD mice.

Material and Methods

Animals

All experiments were performed in compliance with the Guide for the Care and Use of Laboratory Animals and were approved by the University of Missouri Animal Care. Male and female C57BL/6J (Control) and B6.129P2-IL-10tm1Cgn/J ($IL10^{-/-}$, IBD) mice (1–8.5 months old), originally obtained from the Jackson Laboratory were bred and housed at the University of Missouri in a 12:12 light:dark cycle and received standard chow and water. Before experimentation, mice were anesthetized via intraperitoneal injection of ketamine-xylazine (100 mg/kg/5mg/kg). Following tissue dissection and extraction, mice were euthanized via cardiac exsanguination.

Bacterial Cultivation and Inoculation

Helicobacter hepaticus was grown on 5% sheep blood agar plates containing Brucella broth with 5% fetal bovine serum for 48 h at 37°C in a microaerobic chamber with 90% N_2, 5% H2, and 5% CO_2. At 2- and 4-days post-weaning, the IBD mice received *H. hepaticus* suspended in 0.5 mL Brucella broth via gastric gavage. Non-gavaged C57Bl/6J mice served as the Control group. Mice were then allowed to develop disease for 1-240 days before experimentation.

Adipocyte Measurement

For adipocyte measurements of PVAT, first-order mesenteric arteries with surrounding PVAT were hand dissected from Control and IBD mice and fixed in 10% neutral buffered formalin. Tissue was held in place with two layers of biopsy foam pads within a tissue cassette. At the University of Missouri Veterinary Medical Diagnostic Library, 10 μm sections of each sample

were mounted to slides and stained with hematoxylin and eosin. Prepared slides were imaged with a 20X objective on a Nikon E800 microscope, with Nikon Elements software.

Next, the images were analyzed using the Adiposoft plugin for ImageJ, which allowed for automatic counting and measuring of individual adipocytes within the field of view of each image. After automatic counting was done by Adiposoft, manual counting by a lab member was performed to validate the accuracy of adipocyte counts. Cells not included in the automatic count were manually added. In both the automated and manual counts, partial cells at the periphery of each image were excluded from analysis. Representative images were selected from both Control and IBD tissues in order to effectively show the size and density differences between the two groups. Nested t tests were performed to compare group means.

Immunofluorescence

For immunofluorescence studies, time points were as follows (post gavage): 1, 5, 10, 20, 40, 80, 120, 160, and 240 days. Mice were anesthetized with an intraperitoneal injection of ketamine xylazine for subsequent dissection and experimentation. First and second order mesenteric arteries with attached PVAT were hand-dissected in cold physiological saline solution as previously described (Norton et al., 2021). First order MAs with attached PVAT were pinned using a 50-µm wire in a 24-well plate coated with Sylgard. For immunolabelling, all mesenteric arteries with PVAT were pinned intact. The tissue was fixed in 4% paraformaldehyde for 20 minutes, blocked and permeabilized for 60 min with Phosphate-buffered saline containing 1% bovine serum albumin and 0.1% Triton X-100 and incubated overnight in the following primary antibody solutions: CD68 (M1 macrophages), CD206 (M2 Macrophages), and F4/80 (all macrophages) (Table 1A - Antibodies). Tissues were then blocked again for 60 min, incubated in secondary antibodies for 90 min, and mounted on slides. Control experiments included secondary-

only and antibody-free controls to account for nonspecific labeling and autofluorescence (Data not shown). Vendor details and concentrations for all antibodies are listed in Table 1A.

Slides were imaged using a Leica TCS SP8 confocal laser-scanning microscope (Leica Microsystems). Fluorescence for each antibody was sequentially imaged at 1024x1024 pixels using a 25x water immersion objective (NA=0.95) and 1 μm Z-slices through the tissue samples. Similar laser power and gain settings were used on both the control and IBD arteries to facilitate comparison. F4/80, CD86 and CD206 fluorescence was quantified by measuring the fluorescence area of each label in maximum z-projections using ImageJ. Maximum-intensity z-projections were created separately for each channel and converted to binary images with thresholds set to eliminate background fluorescence. First, Maximum z-projections of each channel were exported from LASX and imported to Image J. Background was adjusted to remove non-specific fluorescence. Specifically, the black level (minimum) was increased from 0 to ~30 (on the 0–255 gray level scale) to remove the low-level adipocyte autofluorescence without eliminating the much brighter signal from labeled macrophages. Binary images were generated from these adjusted images. From the binary image, the ImageJ "measure" feature was used to determine the percent fluorescent area, the total fluorescent area fraction within the entire image. Images that could not be adequately adjusted were excluded from analysis. Images were excluded from analysis due to uncorrectable auto-fluorescent background, immunofluorescent non-biological fibers or dust on tissue samples, or poor image quality. No more than six total images were excluded per group.

Table 1A. Antibodies

Target antigen	Vendor	Catalog #	Concentration
CD206 (Goat)	R&D Systems	FAB2535P	1:250
CD68 (Mouse)	Invitrogen	14-0681-82	1:500
F4/80 (Rat) Flow Cytometry Stain (555-conjugated)	Invitrogen	11-4801-81	1:250
Chicken-anti-rat Alexa Fluor 488 (used w/ F4/80)	Invitrogen	A-21470	1:50
Goat-anti-mouse Alexa Fluor 647 (used w/ CD68)	Invitrogen	51-0689-42	1:50

Table 1B. Drugs, Solutions, and Reagents

Name	Vendor or Source	Catalog Number	Concentration(s)
PBS (Phosphate Buffered Saline)	Sigma	P3813	1X
Triton X 100	Sigma	C100	0.1%
Paraformaldehyde	Sigma	1004960700	4%
Neutral Buffered Formalin	Sigma	HT501128	10%

Table 1C. Other relevant supplies and equipment

Name	Vendor or Source	Catalog Number	Other Information
ProLong Gold mounting media	ThermoFisher Scientific	P10144	
BBL Brucella Broth	BD Difco	211088	
Fetal Bovine Serum	MilliporeSigma	F0926	
5% Sheep blood agar plates	Hardy Diagnostics	A10	
Wiretrol II pipette	Drummond Scientific Company	5-000-2100	For transferring vessel segments
Sylgard 184	MilliporeSigma	761036	

Statistical Analysis

All data were statistically analyzed in Graphpad Prism 9, with statistical significance measured at $p<0.05$. For adipocyte size and density measurements, Data were analyzed via nested t test to account for multiple samples taken per mouse. Overall, these data included 6-12 images/sample taken from 3 PVAT samples and 3 mice per group. Frequency histograms for adipocyte size were generated with bin widths of 200 and a range of 600-2800. Histograms for adipocyte density were generated with bin widths of 5 and a range of 35-125. Ranges for each were set as recommended in Graphpad Prism 9. For the time-point study, 4 mice were used per group in each timepoint. Four PVAT samples were taken from each mouse, and 8 images were generated from each sample. To compare macrophage populations in Control vs IBD within the same timepoints, a nested one-way ANOVA with Sidak corrections for multiple comparisons was used. The use of nested statistical methods accounts for the potential of pseudo replication from multiple samples per mouse. To compare changes in macrophage populations across all timepoints in Control vs. IBD mice, a two-way ANOVA with Tukey's correction was utilized for comparison across timepoints. No data points were excluded from analysis as outliers.

Results

PVAT undergoes structural changes during IBD progression

Our previous studies found that PVAT undergoes functional changes during onset of IBD (Figure 1). Here, measurements of mesenteric artery PVAT adipocyte size and density show that the structure of the adipocytes found within PVAT also go through a transformation with IBD. (Figure 2-4). Representative images were chosen from IBD and Control samples (Figure 2). Adipocytes were larger in Control vs IBD (1926±51 vs 1018±32 μm^2, Figure 3) with decreased density (50.7 ±1.0 vs 79.4 ±2.0 cells/field, Figure 4). Thus, IBD leads to smaller, more densely packed adipocytes within PVAT of mesenteric arteries. Frequency histograms for size and density also show that IBD is also associated with an increase in the distribution of size and density (Figure 3B and 4B) vs Control. As shown in the representative images (Figure 2), PVAT from IBD mice typically had greater amounts of both henatoxylin (purple) and eosin (pink) staining, suggesting a larger stromal vascular fraction in PVAT with IBD.

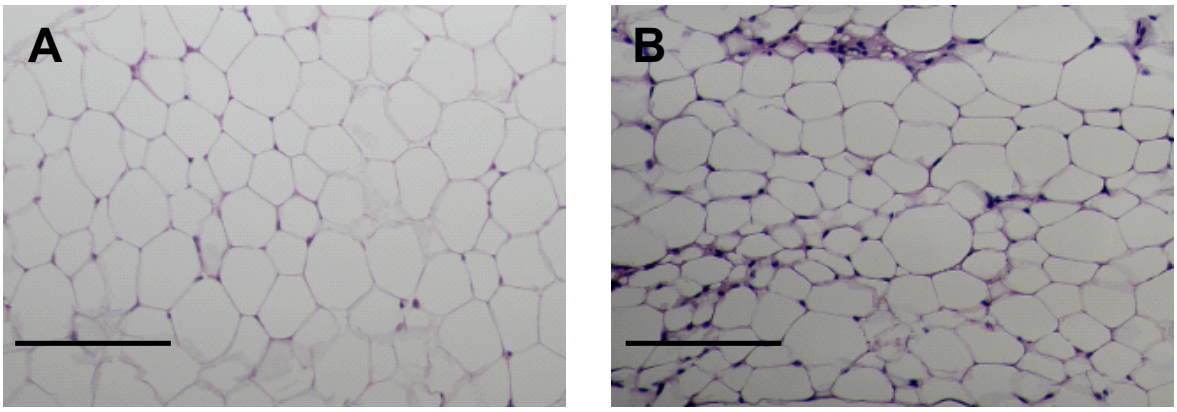

Figure 2. ***Representative images of mesenteric PVAT from Control and IBD mice.*** Images are representative 10 μm slices of H&E-stained PVAT from (A) Control and (B) IBD mice. Scale bar = 100 μm. FOV = 490 by 490 μm

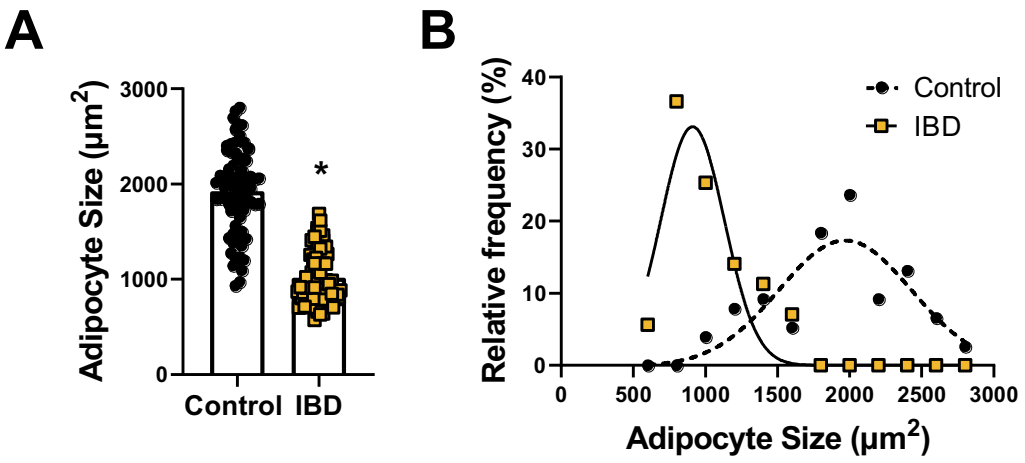

Figure 3. ***Mesenteric PVAT adipocyte size decreases with IBD.***
A. Summary Data are mean ± SE for adipocyte size in Control (black) vs IBD (gold) PVAT samples. B. Frequency distribution histogram of adipocyte size in Control vs. IBD samples. N= 71 (Control) or 76 (IBD) images analyzed from 16 PVAT sample each in 4 mice per group. * = $p < 0.05$ via nested t-test.

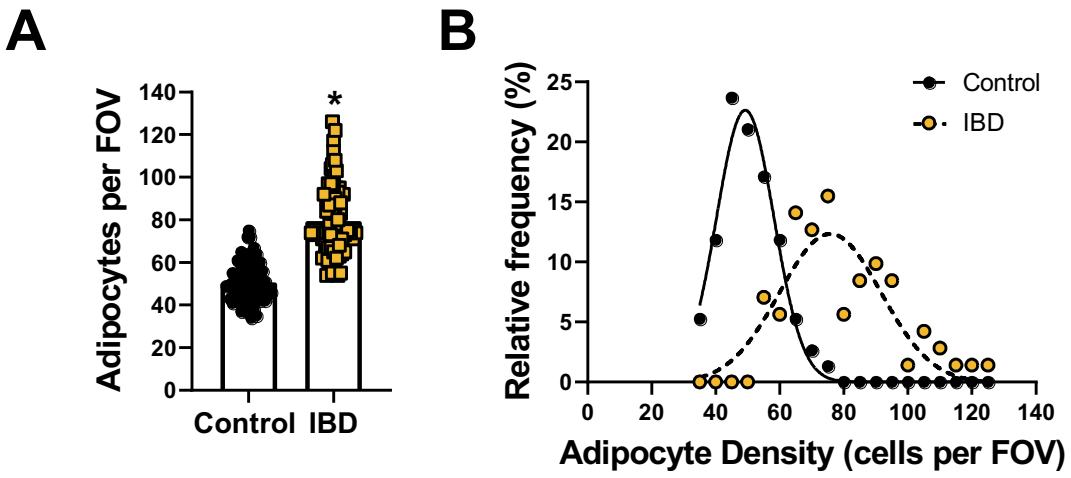

Figure 4. ***Mesenteric PVAT adipocyte density increases with IBD.***
A. Summary Data are mean ± SE for adipocyte density (cells per field of view, FOV give dimensions) in Control (black) vs IBD (gold) PVAT samples. B. Frequency distribution histogram of adipocyte density in Control vs. IBD samples. N= 71 (Control) or 76 (IBD) images analyzed from 16 PVAT sample each in 4 mice per group. * = $p < 0.05$ via nested t-test.

Timepoint Study: PVAT macrophage population changes throughout IBD pathogenesis

The purpose of the time point study was to define total, M1 and M2-like macrophages in mesenteric PVAT throughout the pathogenesis of IBD. Thus, the data provide insight into when macrophage proliferation occurs during disease development. Mesenteric PVAT from Control and IBD mice was labeled for F4/80+ (total macrophages), CD68+ (M1-like macrophages) and CD206+ (M2-like macrophages) at each of the following days post-gavage: 1, 5, 10, 20, 40, 80, 160, and 240. All numerical data result from the quantitation of confocal images taken from PVAT samples from Control and IBD mice at each timepoint.

Early timepoints: increased total, M1 and M2 macrophages

The Day 1 timepoint was associated with a significant increase in F4/80 (total), CD206 (M2-like), and CD68 (M1-like) fluorescence (Figures 5-6). F4/80 area increased (10.62±0.29% vs 5.3±0.08%) in IBD vs Control. CD206 also increased (3.62±0.11% vs 2.49±0.13%) in IBD vs Control, indicating an increase in M2-like macrophages. CD68 area increased (4.62±0.11% vs 2.2±0.08%) in IBD vs Control, demonstrating a concurrent increase in M1-like macrophages. (Figure 6A). Nested representation summary data of Day 1 (Figure 6B) shows the same data separated to highlight the technical replicates from each mouse. Nested analysis shows that the observed differences in Control vs IBD samples are still statistically significant when multiple samples per animal are considered.

The trend of increased total, M1 and M2 macrophages in the mesenteric PVAT of IBD mice continued at Day 5 (Figures 7-8). Similar to the Day 1, all three measurements showed significant increases in IBD vs Control: F4/80 was increased (10.36±0.56% vs 5.71±0.2%), CD206 was increased (3.71±0.09% vs 2.59±0.1%), and CD68 was increased (4.18±0.29% vs 2.19±0.08%,

Figure 8A). Similarly, accounting for multiple technical PVAT replicates with nested analysis did not affect the statistical significance of each increase (Figure 8A).

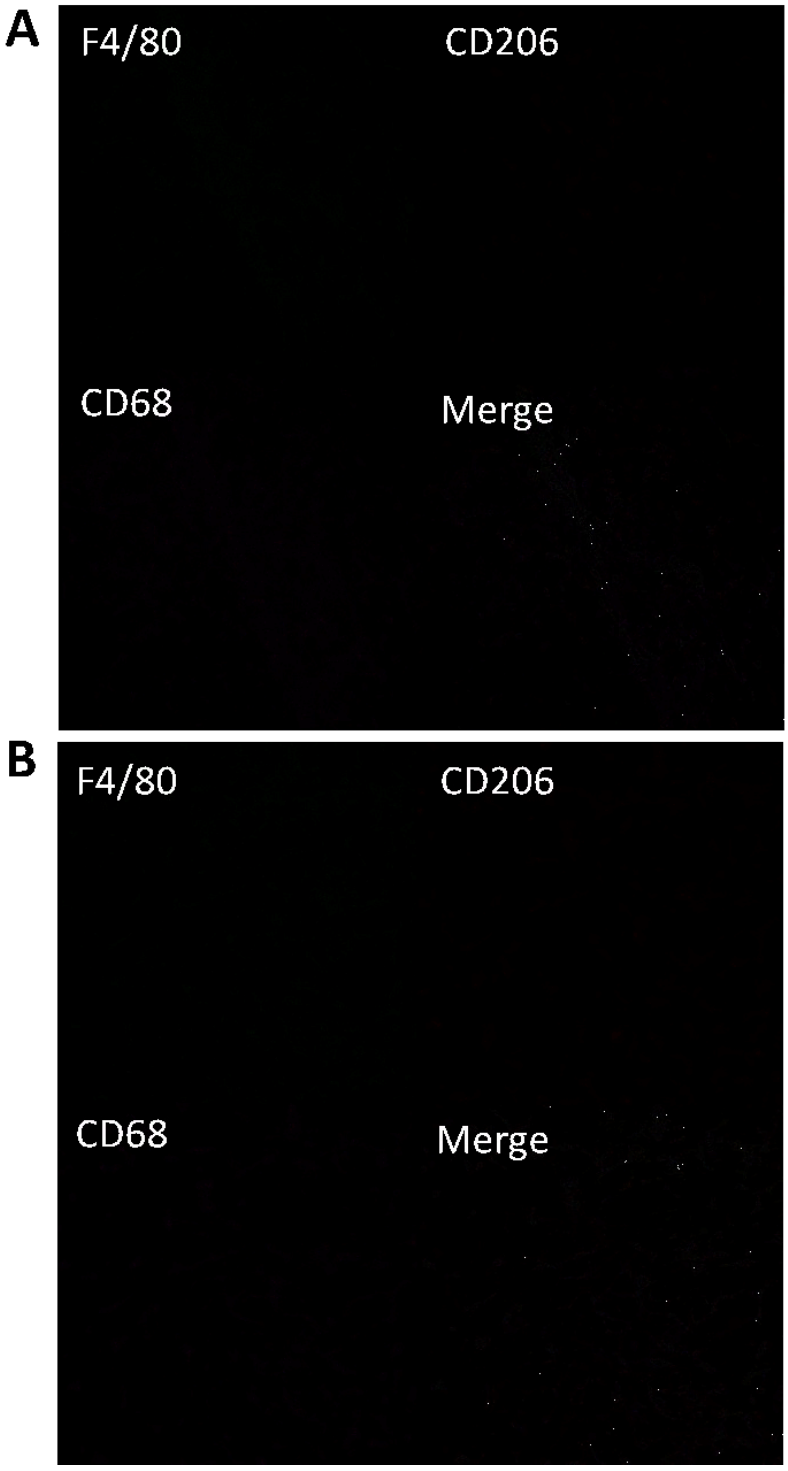

Figure 5. ***Day 1 representative images:*** Images panels are representative maximum z-projections through the mesenteric PVAT labeled for total (F4/80+, upper left, green), M2-like (CD206+, upper right, red), and M1-like (CD68+, lower left, magenta) macrophages, along with an overlay of all channels (lower right) in (A) Control and (B) IBD mice. All images are 486 x 486 μm.

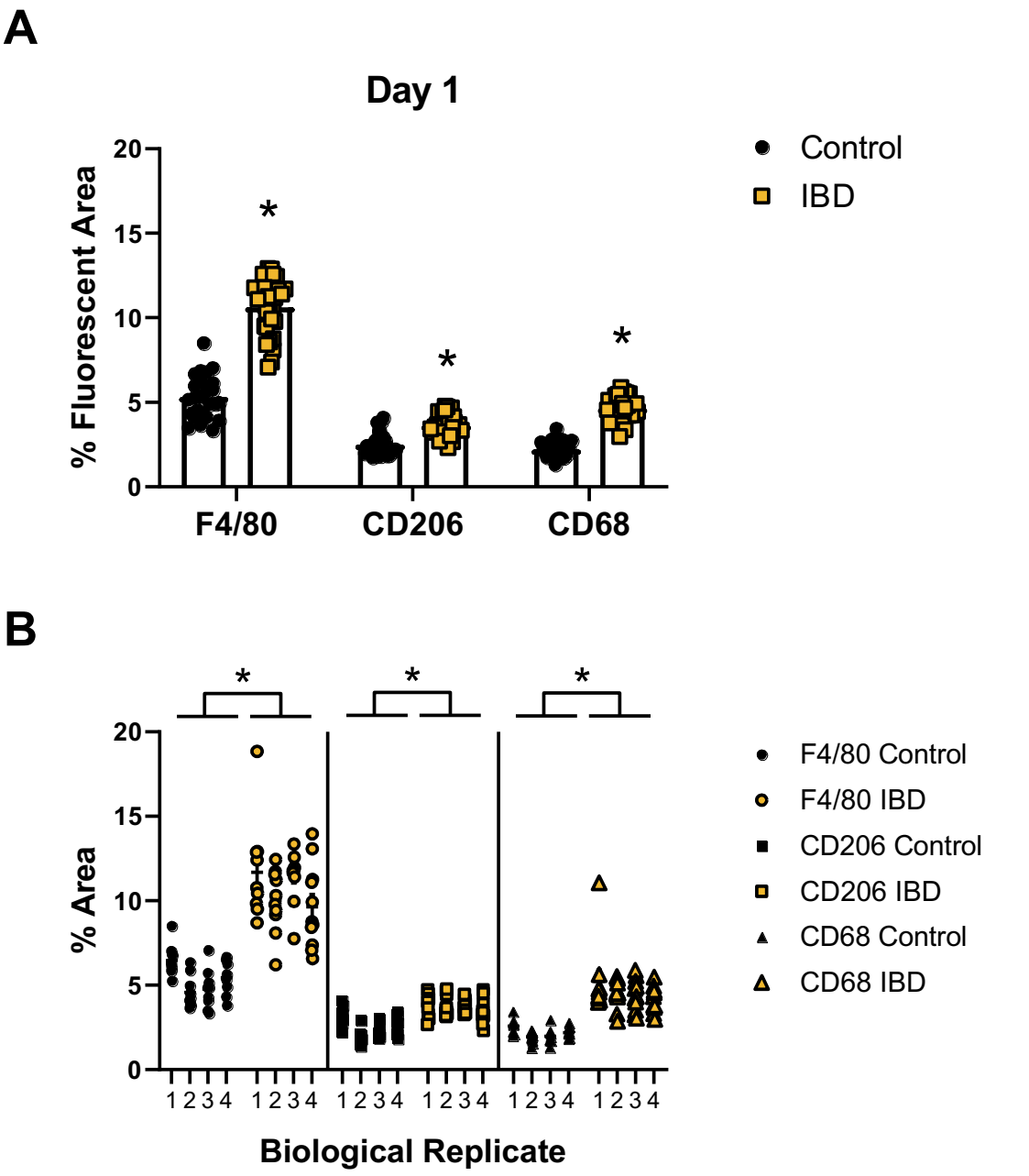

Figure 6. ***Total, M1 and M2 macrophages increase in mesenteric PVAT at Day 1 of IBD development.*** A. Fluorescent area percentage of F4/80, CD206, and CD68. Data are means +/- SE in Control vs IBD PVAT samples labeled for total (F4/80+), M2-like (CD206+), M1-like (CD68+) macrophages. B. Summary data from A reflecting images from each biological replicate for F4/80, CD206, and CD68. For all data * = $P < 0.05$ for control vs IBD via nested one-way ANOVA with Sidak correction. N= 26 (control) or 32 (IBD) analyzed images from 2 PVAT sections in each of 4 mice per group.

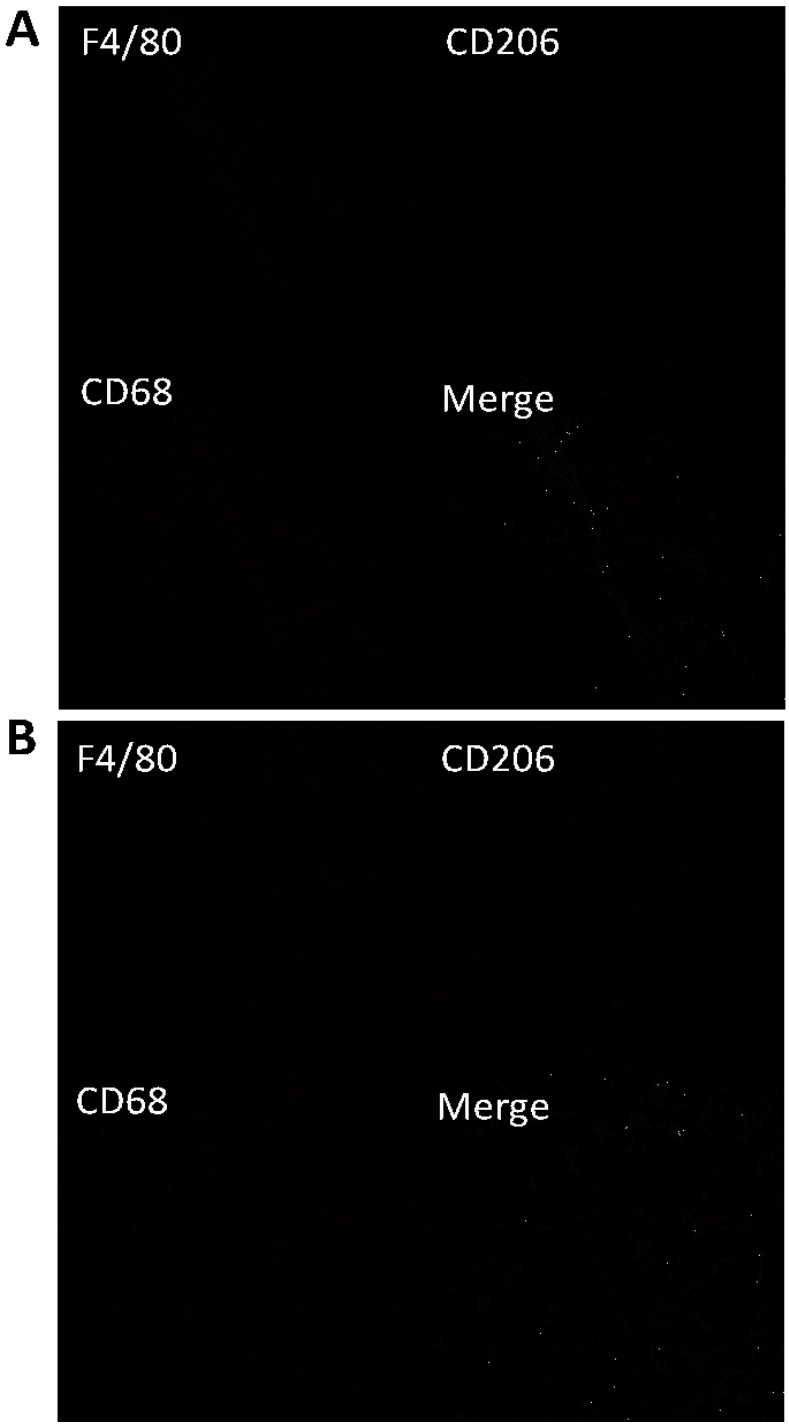

Figure 7: ***Day 5 representative images:***
Images panels are representative maximum z- projections through the mesenteric PVAT labeled for total (F480+, upper left, green), M2-like (CD206+, upper right, red), and M1-like (CD68+, lower left magenta) macrophages, along with an overlay of all channels (lower right) in (A) Control and (B) IBD mice. All images are 486 x 486 μm.

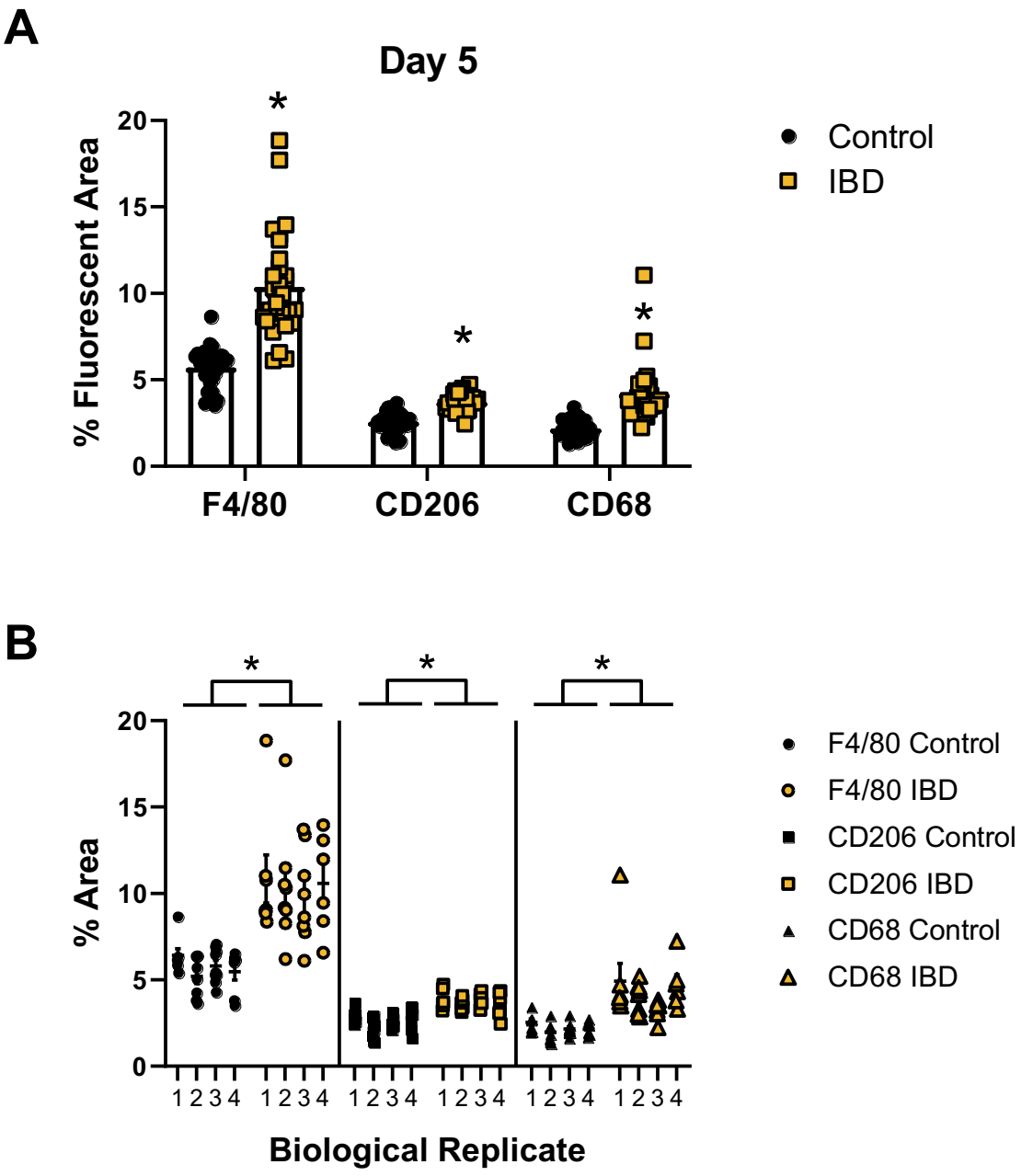

Figure 8. ***Total, M1 and M2 macrophages increase in mesenteric PVAT at Day 5 of IBD development.*** A. Fluorescent area percentage of F4/80, CD206, and CD68. Data are means +/- SE in Control vs IBD PVAT samples labeled for total (F4/80+), M2-like (CD206+), M1-like (CD68+) macrophages. B Summary data from A reflecting images from each biological replicate for F4/80, CD206, and CD68. For all data * = $P < 0.05$ for control vs IBD via nested one-way ANOVA with Sidak correction. N= 30 (control) or 28 (IBD) analyzed images from 2 PVAT sections in each of 4 mice per group.

Middle timepoints: Increased total and M1-like, but not M2-like macrophages with IBD

Like Days 1 and 5, Day 10 was associated with an increase in PVAT fluorescent labeling for total (F4/80) and M1 (CD68) macrophages (Figures 9-10). F4/80 was increased (9.86±0.28% vs 5.3±0.08%) in IBD mice vs Control, and CD68 was increased (3.39±0.11% vs 2.18±0.07%) in IBD vs Control (Figure 10A). In contrast to the early timepoints, M2 labeling was no longer significantly different between groups: CD206 staining remained consistent (3.23±0.07% vs 2.86±0.09%) in IBD vs Control (Figure 10A). These changes were statistically significant after correcting for multiple technical replicates (Figure 10B).

The pattern observed on Day 10 persisted on Day 20, with increased total and M1, but not M2 macrophage area (Figures 11-12). F4/80 was increased (9.86±0.23% vs 7.56±0.14%) in IBD mice vs Control. CD206 was unchanged between in IBD vs Control groups (3.22±0.14% vs 3.43±0.07%). CD68 was increased (3.46±0.12% vs 2.33±0.08%) in IBD vs Control (Figure 12A). Nested summary data of Day 20 show that the trends seen in the combined data are still statistically significant when multiple samples per animals are accounted for (Figure 12B).

Day 40 was associated with a continuation in significantly increased total and M1, but not M2 macrophages in Control vs IBD samples (Figures 13-14). F4/80 was significantly increased (10.01±0.23% vs 7.56±0.24%) in IBD mice vs Control. CD206 was similar (3.21±0.12% vs 3.58±0.13%) in IBD vs Control, and CD68 was increased (3.43±0.06% vs 2.45±0.09%) in IBD vs Control (Figure 13A). Again, technical replicates did not affect these trends, per the nested analysis (Figure 13B). Overall, the data from Days 10-40 suggest that the progression of IBD at this stage may depend on M1 macrophages to a greater extent than M2 macrophages.

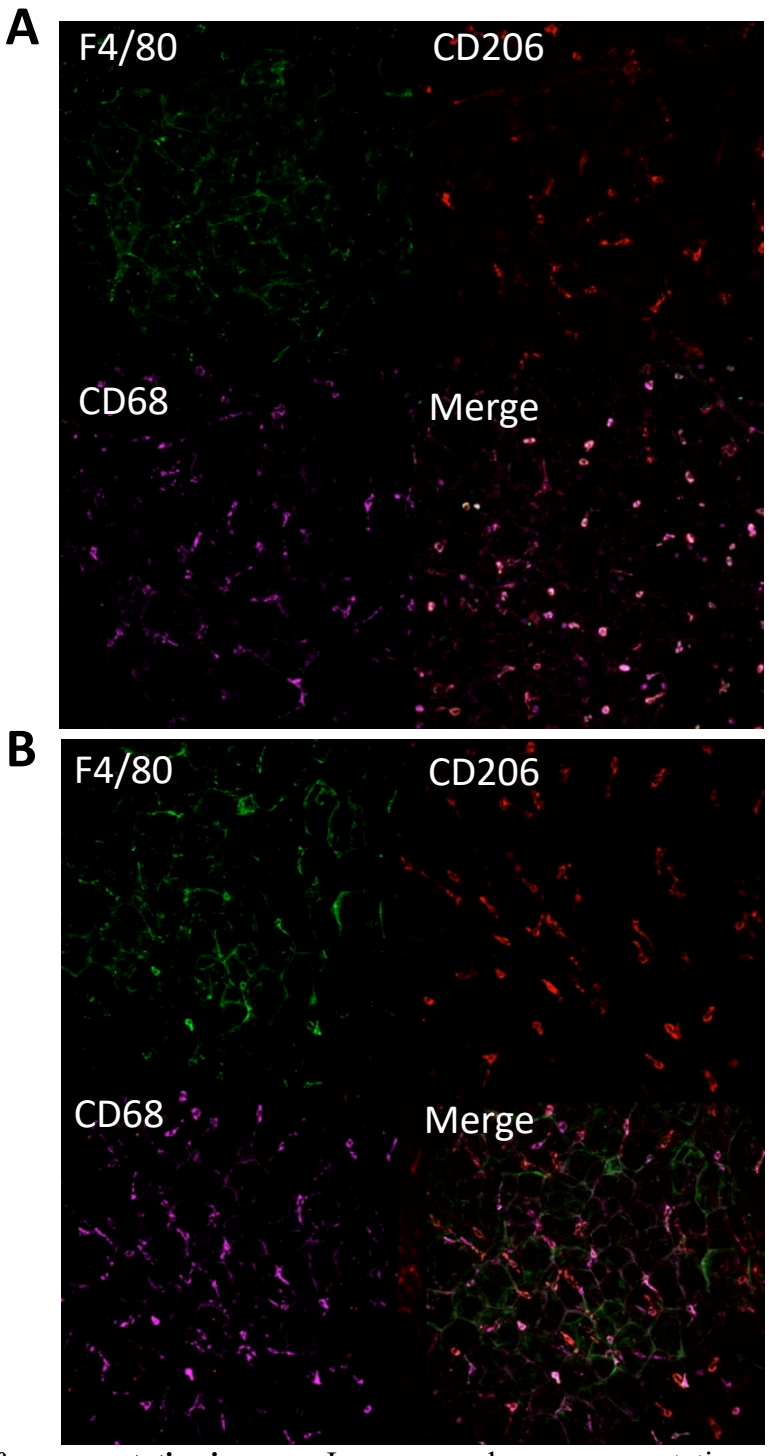

Figure 9. ***Day 10 representative images:*** Images panels are representative maximum z-projections through the mesenteric PVAT labeled for total (F480+, upper left, green), M2-like (CD206+, upper right, red), and M1-like (CD68+, lower left magenta) macrophages, along with an overlay of all channels (lower right) in (A) Control and (B) IBD mice. All images are 486 x 486 μm.

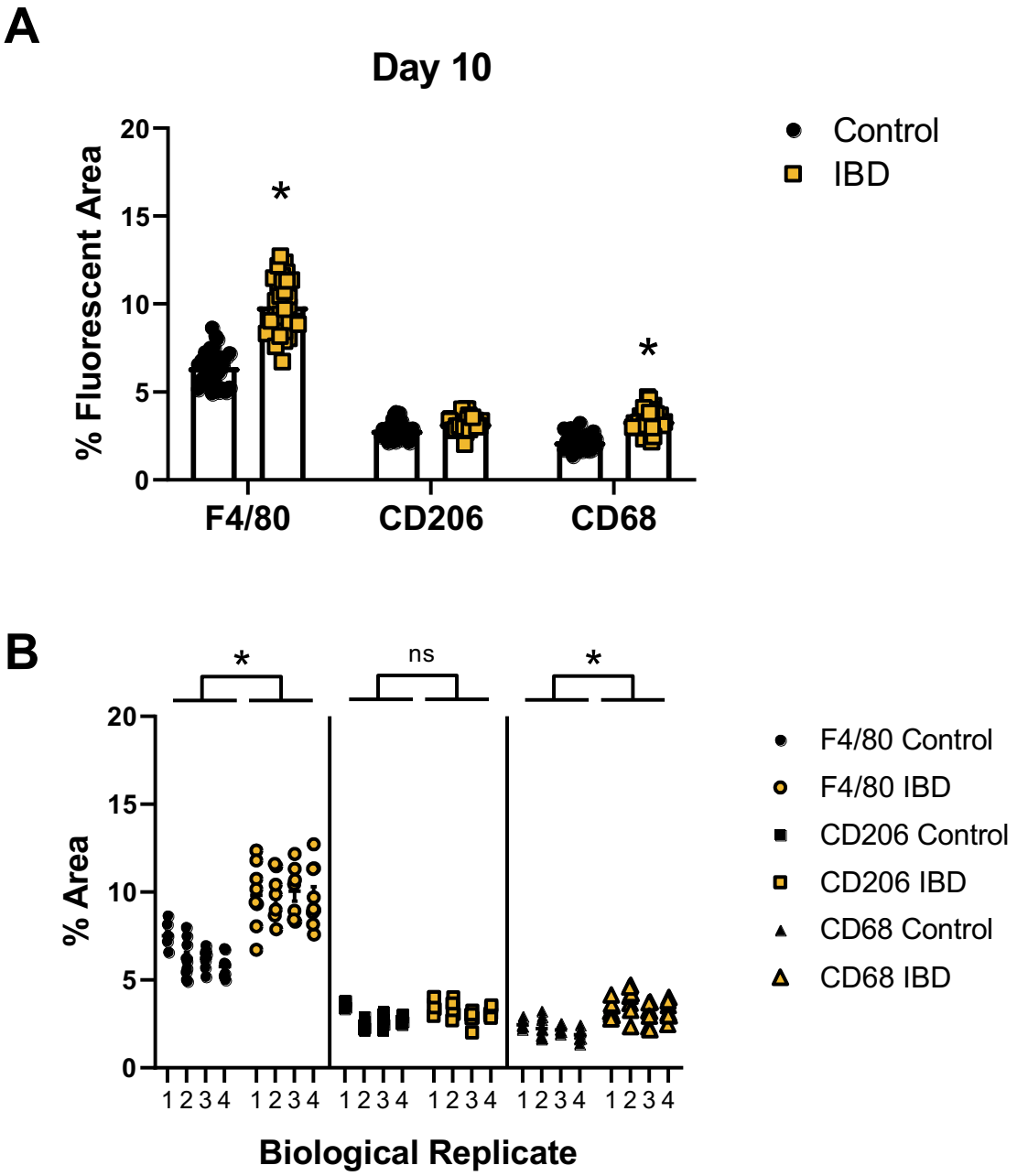

Figure 10. ***Total and M1, but not M2 macrophages increase in mesenteric PVAT at Day 10 of IBD development.*** A. Fluorescent area percentage of F4/80, CD206, and CD68. Data are means +/- SE in Control vs IBD PVAT samples labeled for total (F4/80+), M2-like (CD206+), M1-like (CD68+) macrophages. B Summary data from A reflecting images from each biological replicate for F4/80, CD206, and CD68. For all data * = $P < 0.05$ for control vs IBD via nested one-way ANOVA with Sidak correction. N= 31 (control) or 32 (IBD) analyzed images from 2 PVAT sections in each of 4 mice per group.

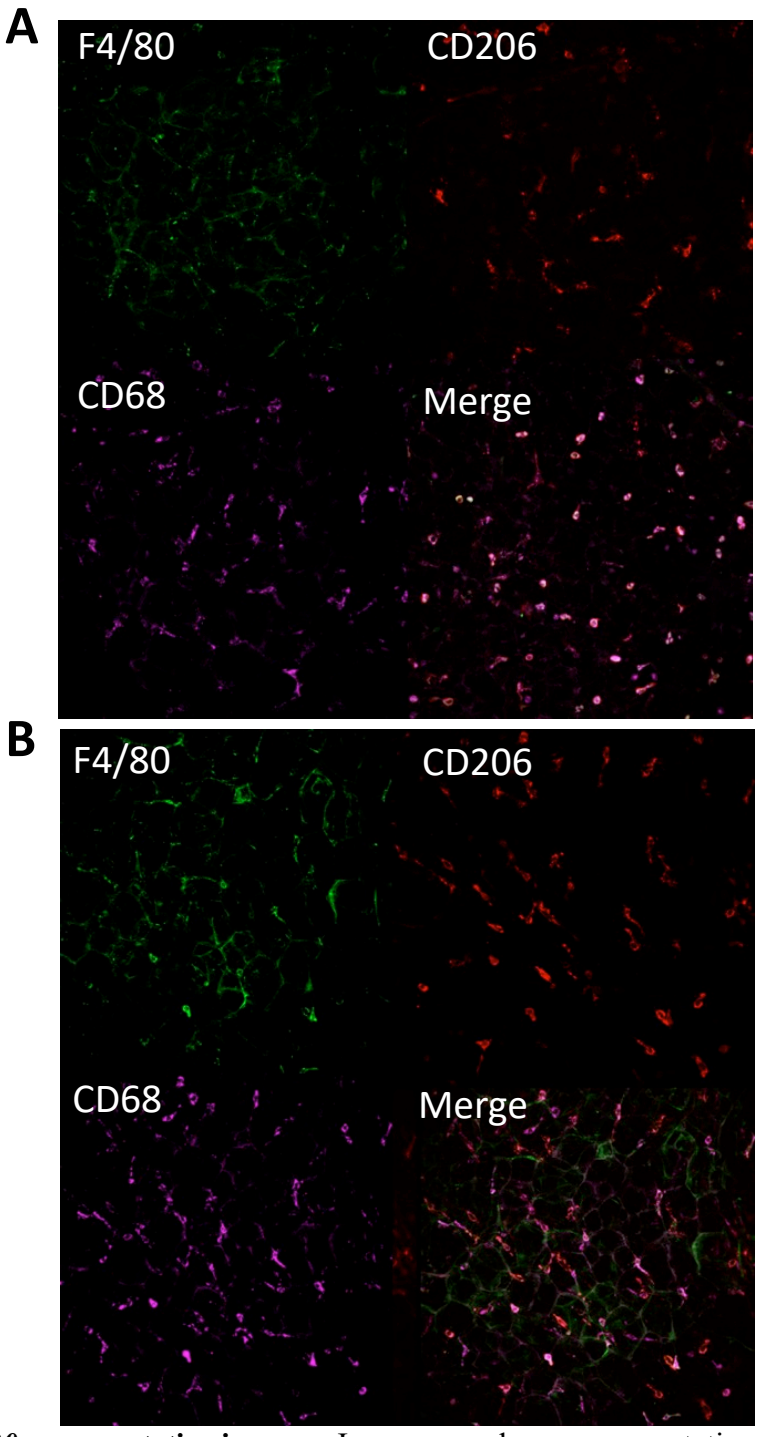

Figure 11. ***Day 20 representative images:*** Images panels are representative maximum z-projections through the mesenteric PVAT labeled for total (F480+, upper left, green), M2-like (CD206+, upper right, red), and M1-like (CD68+, lower left magenta) macrophages, along with an overlay of all channels (lower right) in (A) Control and (B) IBD mice. All images are 486 x 486 μm.

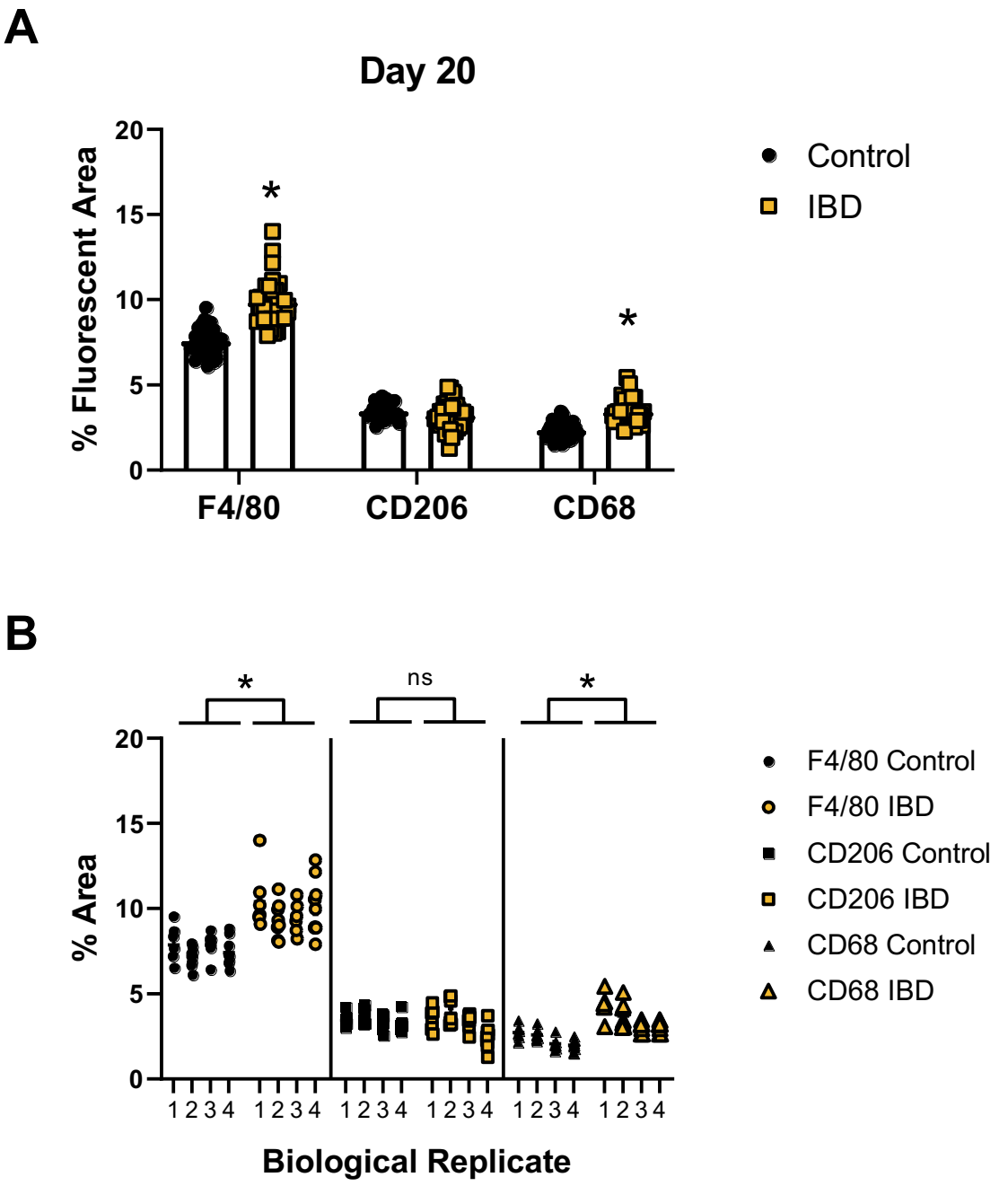

Figure 12. ***Total and M1, but not M2 macrophages increase in mesenteric PVAT at Day 20 of IBD development.*** A. Fluorescent area percentage of F4/80, CD206, and CD68. Data are means +/- SE in Control vs IBD PVAT samples labeled for total (F4/80+), M2-like (CD206+), M1-like (CD68+) macrophages. B Summary data from A reflecting images from each biological replicate for F4/80, CD206, and CD68. For all data * = $P < 0.05$ for control vs IBD via nested one-way ANOVA with Sidak correction. N= 32 (control) or 33 (IBD) analyzed images from 2 PVAT sections in each of 4 mice per group.

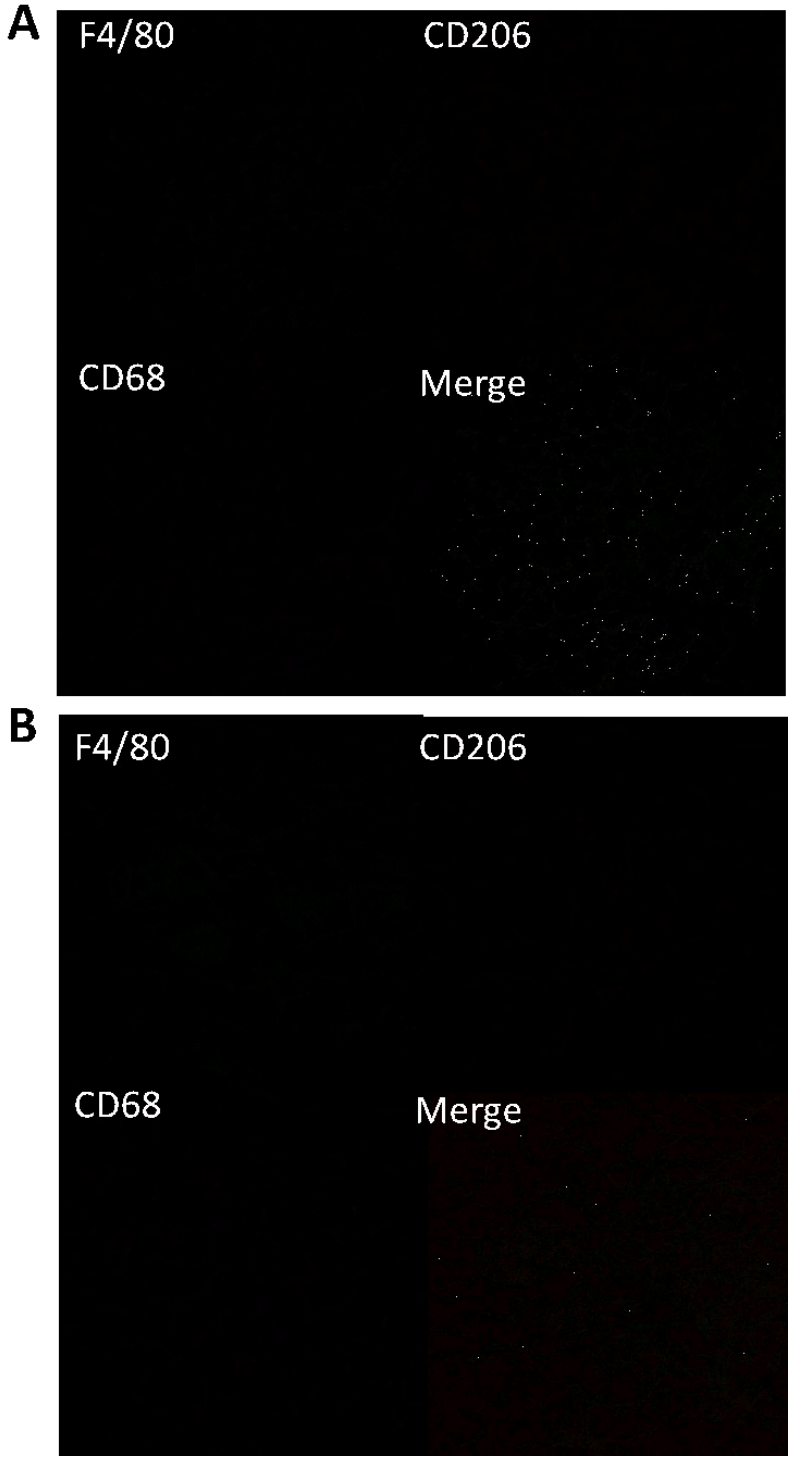

Figure 13. ***Day 40 representative images:*** Images panels are representative maximum z-projections through the mesenteric PVAT labeled for total (F480+, upper left, green), M2-like (CD206+, upper right, red), and M1-like (CD68+, lower left magenta) macrophages, along with an overlay of all channels (lower right) in (A) Control and (B) IBD mice. All images are 486 x 486 μm.

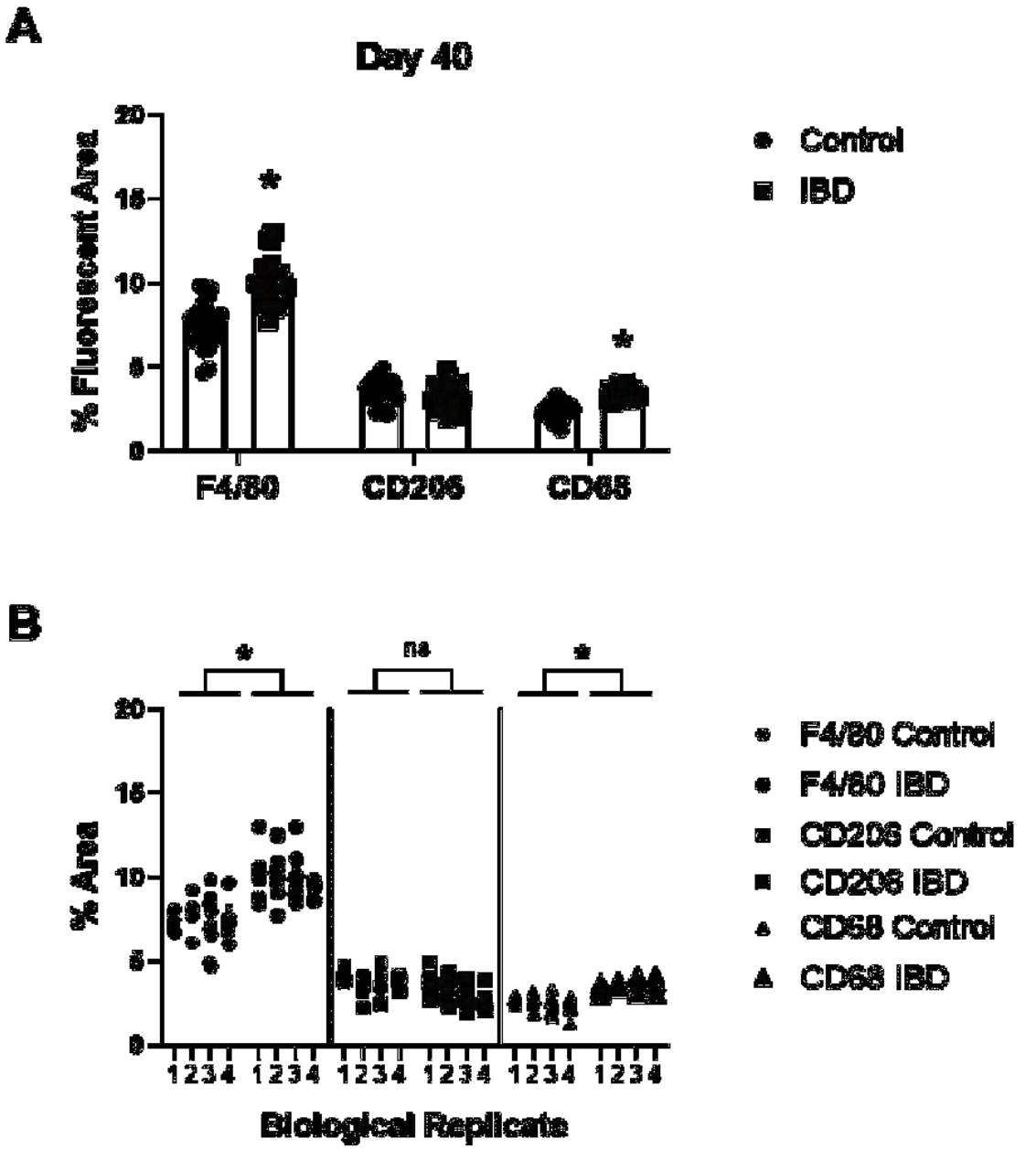

Figure 14. ***Total and M1, but not M2 macrophages increase in mesenteric PVAT at Day 40 of IBD development.*** A. Fluorescent area percentage of F4/80, CD206, and CD68. Data are means +/- SE in Control vs IBD PVAT samples labeled for total (F4/80+), M2-like (CD206+), M1-like (CD68+) macrophages. B Summary data from A reflecting images from each biological replicate for F4/80, CD206, and CD68. For all data * = $P < 0.05$ for control vs IBD via nested one-way ANOVA with Sidak correction. N= 28 (control) or 31 (IBD) analyzed images from 2 PVAT sections in each of 4 mice per group.

Late timepoints: increased total and M1 macrophages, decreased M2 macrophages

Like Day 40, Day 80 in IBD mice was associated with an increase in PVAT fluorescent labeling for total (F4/80) and M1 (CD68). F4/80 was increased (10.06±0.24% vs 8±0.23%) in IBD mice vs Control and CD68 was increased (4.22±0.16% vs 2.21±0.07%) in IBD vs Control. In contrast to both early and middle timepoints, M2 labeling was significantly decreased ~~between~~ with IBD: CD206 staining decreased (2.48±0.06% vs 3.68±0.16%) in IBD vs Control (Figure 16A). These changes were statistically significant after correcting for multiple technical replicates (Figure 16B).

Day 160 was associated with an increase in PVAT fluorescent labeling for total (F4/80) and M1 (CD68) (Figures 17-18). F4/80 was increased (10.45±0.27% vs 8.35±0.21%) in IBD mice vs Control and CD68 was increased (5.29±0.29% vs 2.69±0.08%) in IBD vs Control. However, in contrast to the previous timepoint (Day 80). M2 (CD206) macrophages were not significantly different: CD206 was similar (2.85±0.11% vs 3.71±0.16%) in IBD vs Control (Figure 18A). Nested summary data of Day 160 show that the trends seen in the combined data are still statistically significant when multiple samples per animals are accounted for (Figure 18B).

Day 240 trends reflect that of Day 80 (Figures 19-20). F4/80 was increased (11.79±0.51% vs 8.63±0.29%) in IBD mice vs Control and CD68 was increased (5.33±0.2% vs 2.42±0.08%) in IBD vs Control. CD206 was decreased (2.82±0.19% vs 4.02±0.2%) in IBD vs Control (Figure 20A). Again, technical replicates did not affect these trends, per the nested analysis (Figure 20B). Overall, the data from Days 80-240 suggest that the progression of IBD at this stage may depend on M1 macrophages and a lack of M2 macrophages and their anti-inflammatory effect.

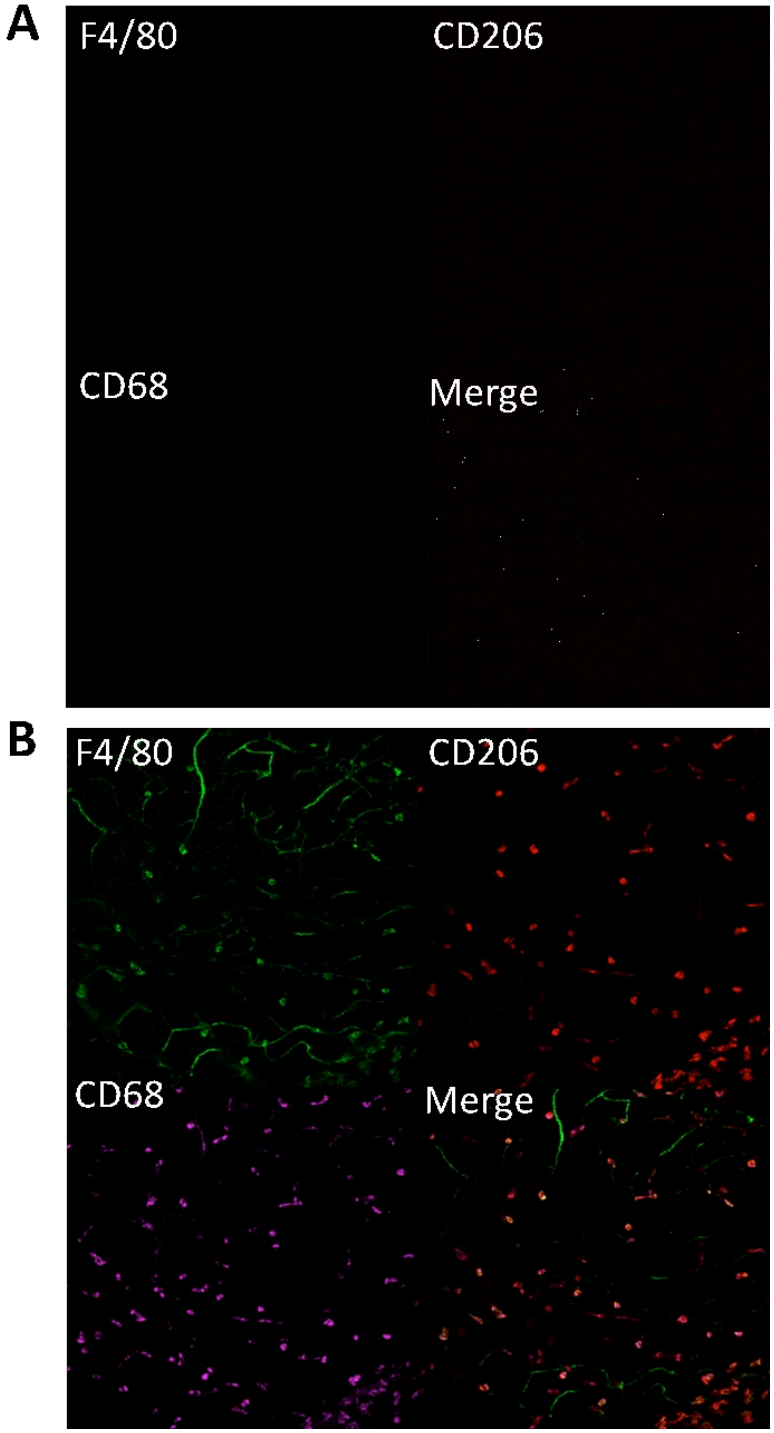

Figure 15. ***Day 80 representative images:*** Images panels are representative maximum z-projections through the mesenteric PVAT labeled for total (F480+, upper left, green), M2-like (CD206+, upper right, red), and M1-like (CD68+, lower left magenta) macrophages, along with an overlay of all channels (lower right) in (A) Control and (B) IBD mice. All images are 486 x 486 μm.

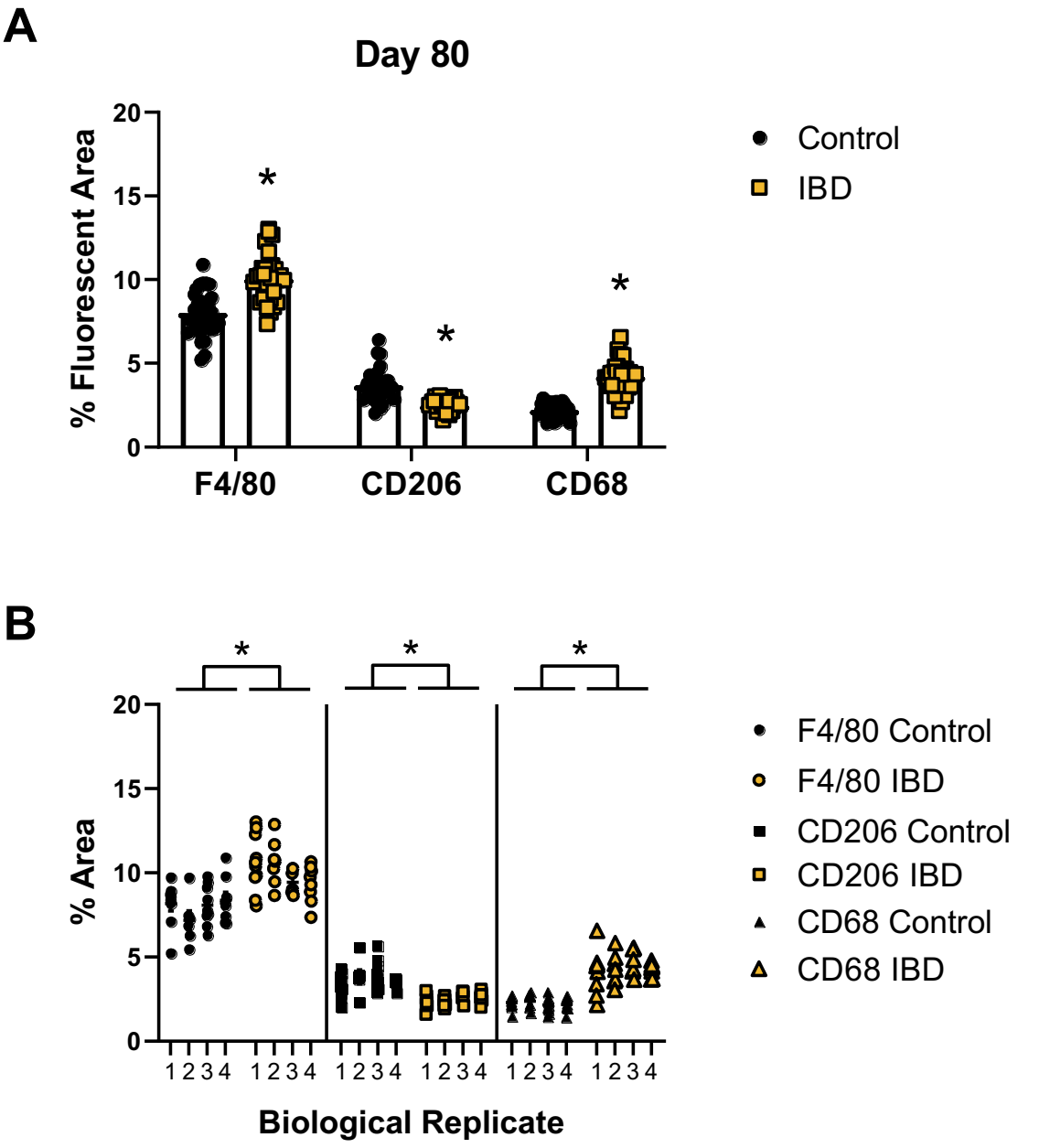

Figure 16. ***Total and M1, and M2 macrophages increase in mesenteric PVAT at Day 80 of IBD development.*** A. Fluorescent area percentage of F4/80, CD206, and CD68. Data are means +/- SE in Control vs IBD PVAT samples labeled for total (F4/80+), M2-like (CD206+), M1-like (CD68+) macrophages. B Summary data from A reflecting images from each biological replicate for F4/80, CD206, and CD68. For all data * = $P < 0.05$ for control vs IBD via nested one-way ANOVA with Sidak correction. N= 32 (control) or 32 (IBD) analyzed images from 2 PVAT sections in each of 4 mice per group.

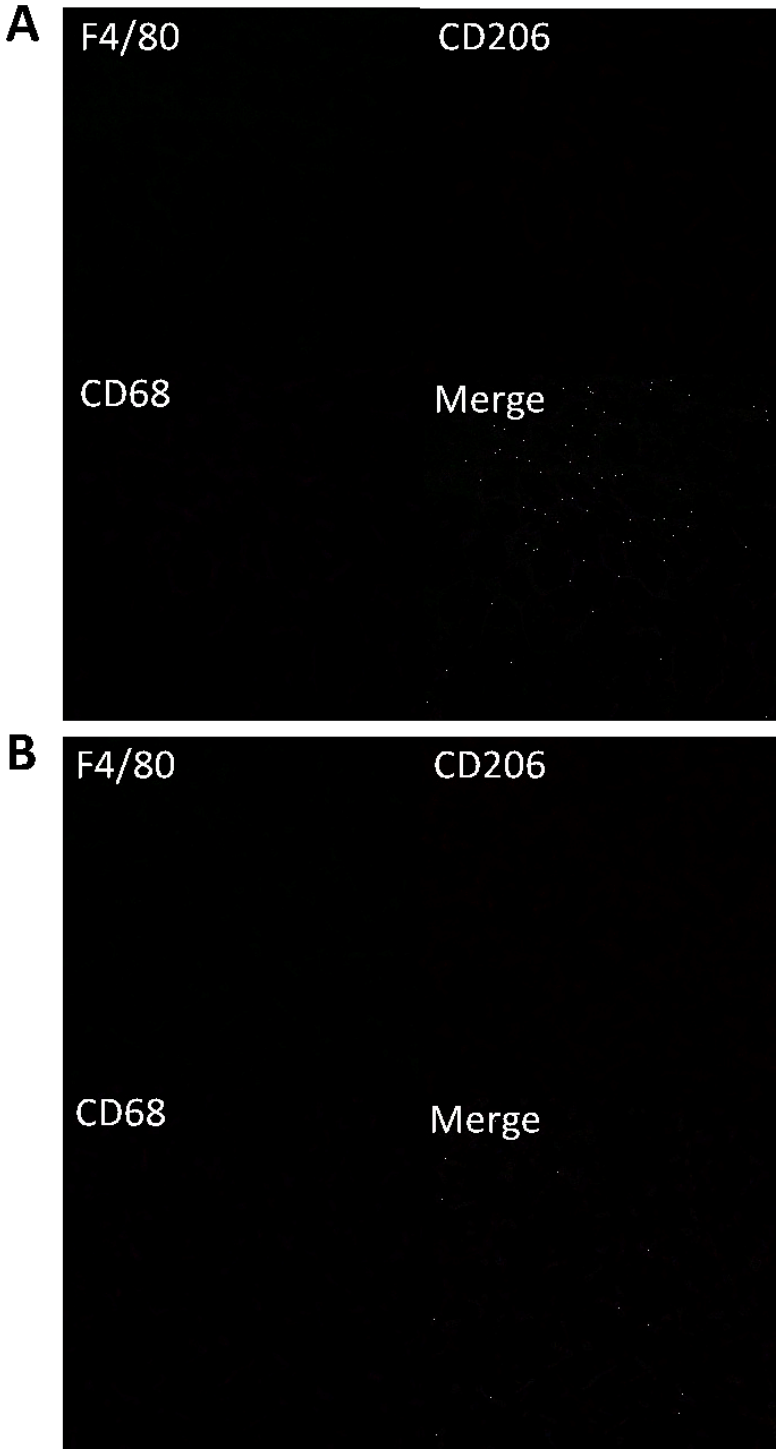

Figure 17. ***Day 160 representative images:*** Images panels are representative maximum z-projections through the mesenteric PVAT labeled for total (F480+, upper left, green), M2-like (CD206+, upper right, red), and M1-like (CD68+, lower left magenta) macrophages, along with an overlay of all channels (lower right) in (A) Control and (B) IBD mice. All images are 486 x 486 μm.

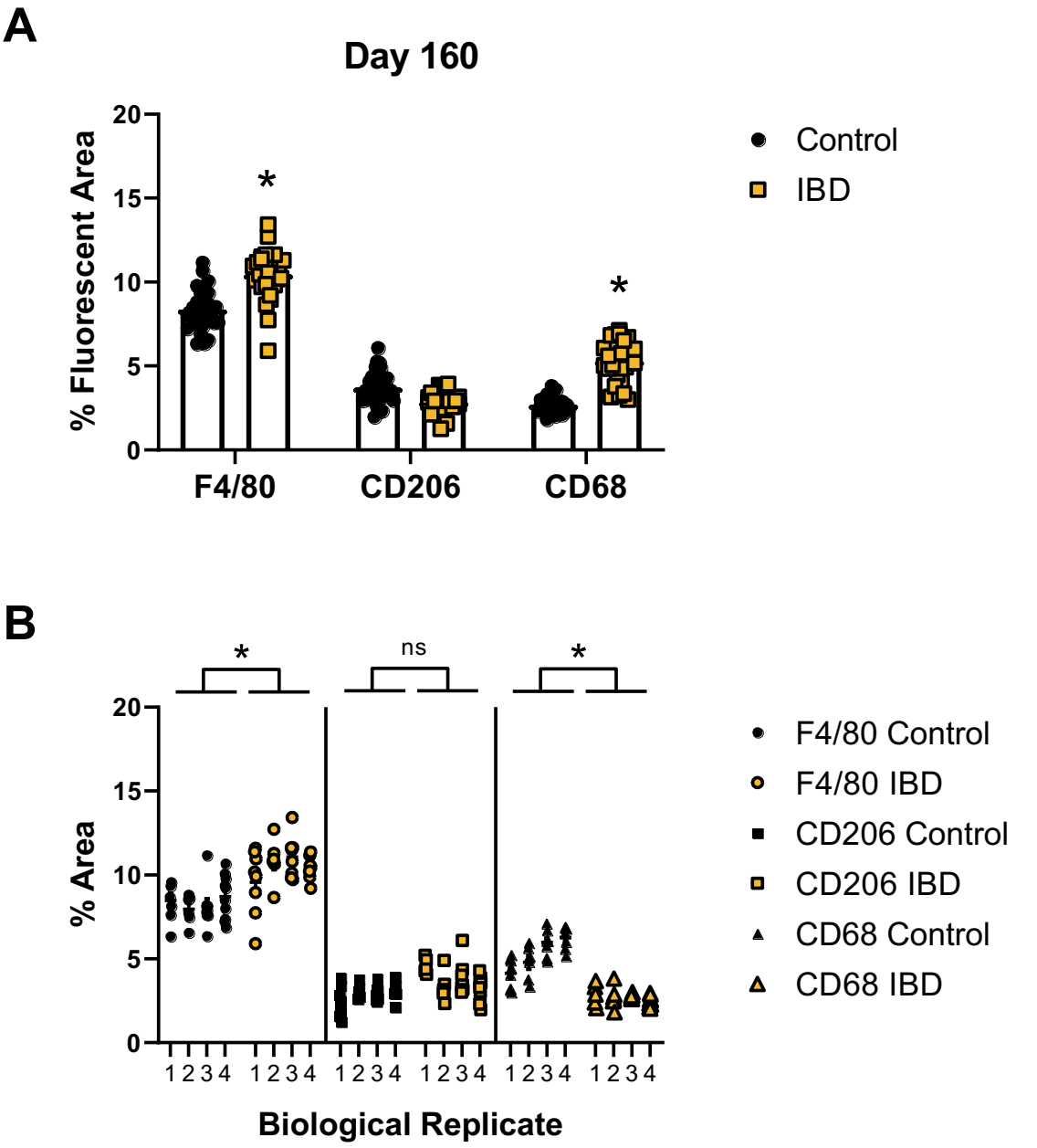

Figure 18. ***Total and M1, and M2 macrophages increase in mesenteric PVAT at Day 160 of IBD development.*** A. Fluorescent area percentage of F4/80, CD206, and CD68. Data are means +/- SE in Control vs IBD PVAT samples labeled for total (F4/80+), M2-like (CD206+), M1-like (CD68+) macrophages. B Summary data from A reflecting images from each biological replicate for F4/80, CD206, and CD68. For all data * = $P < 0.05$ for control vs IBD via nested one-way ANOVA with Sidak correction. N= 31 (control) or 29 (IBD) analyzed images from 2 PVAT sections in each of 4 mice per group.

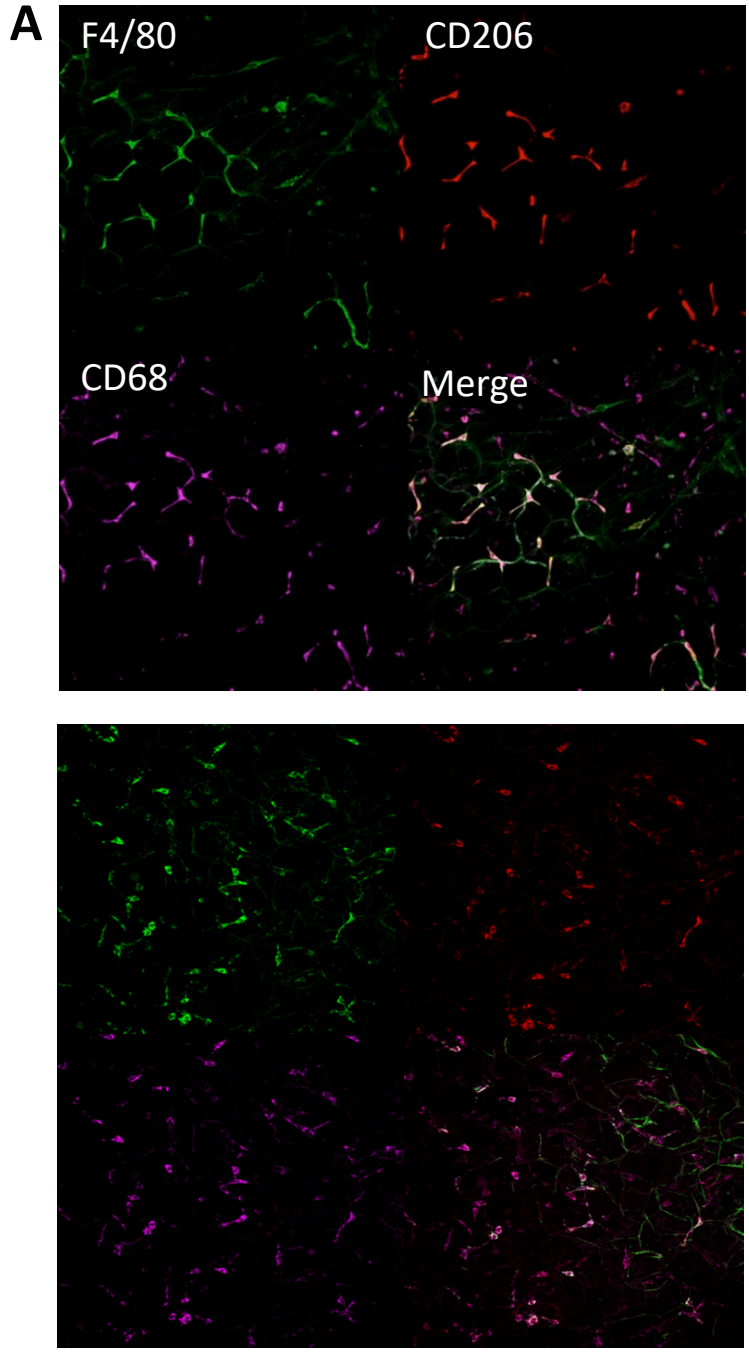

Figure 19. ***Day 240 representative images:*** Images panels are representative maximum z-projections through the mesenteric PVAT labeled for total (F480+, upper left, green), M2-like (CD206+, upper right, red), and M1-like (CD68+, lower left magenta) macrophages, along with an overlay of all channels (lower right) in (A) Control and (B) IBD mice. All images are 486 x 486 μm.

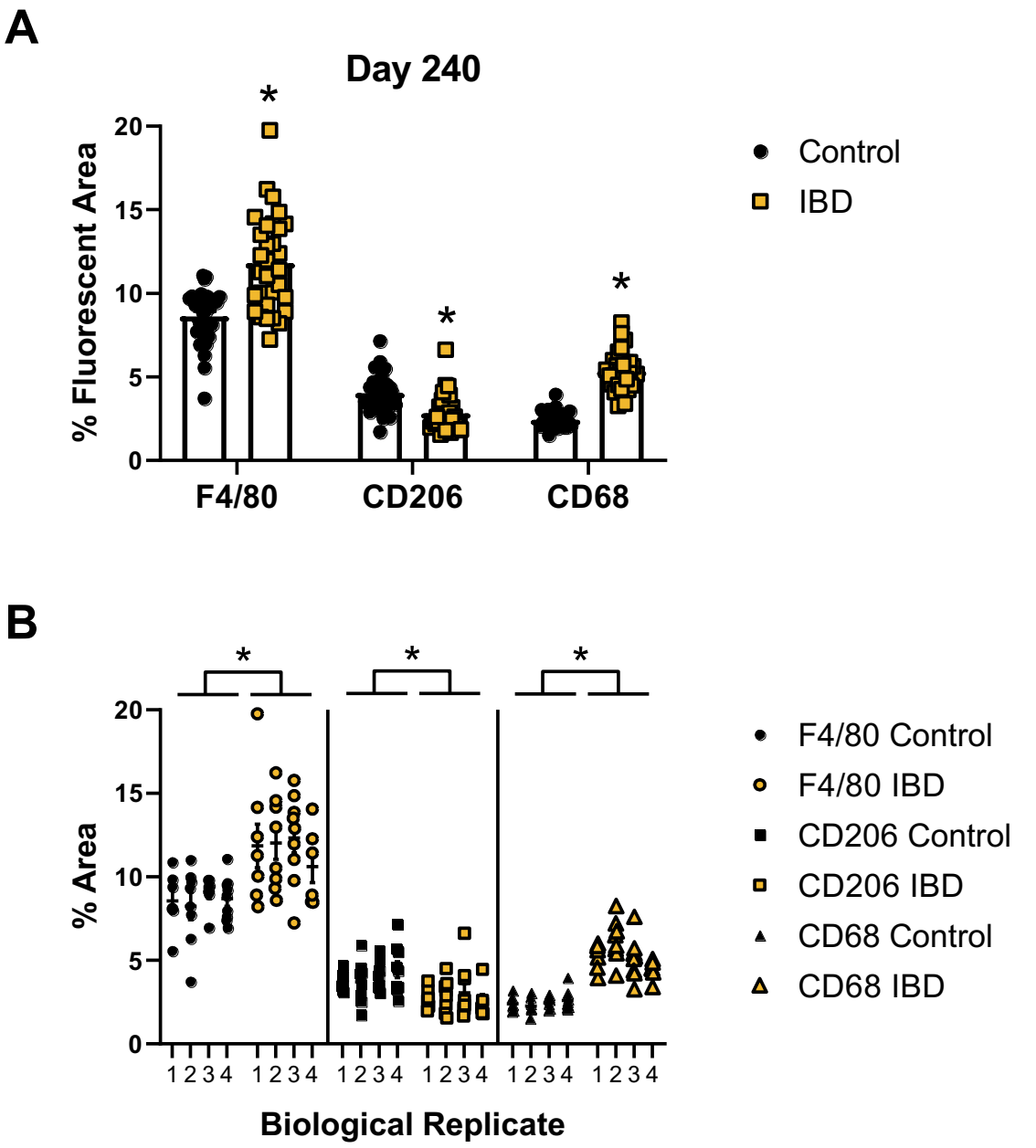

Figure 20. ***Total and M1, and M2 macrophages increase in mesenteric PVAT at Day 240 of IBD development.*** A. Fluorescent area percentage of F4/80, CD206, and CD68. Data are means +/- SE in Control vs IBD PVAT samples labeled for total (F4/80+), M2-like (CD206+), M1-like (CD68+) macrophages. B Summary data from A reflecting images from each biological replicate for F4/80, CD206, and CD68. For all data * = $P < 0.05$ for control vs IBD via nested one-way ANOVA with Sidak correction. N= 32 (control) or 31 (IBD) analyzed images from 2 PVAT sections in each of 4 mice per group.

Trends over time: Increased contribution of M2 vs M1 macrophages during IBD pathogenesis

Understanding IBD-related changes in PVAT macrophages within a single timepoint is important but does not give a global view on how the populations change over time. To display the changes over the full course of the study, we analyzed the data to test for differences from Day 1 to Day 240 of total, M2 and M1-like macrophages (Figure 21). This analysis has the benefit of showing data trends over time both within and between groups, highlighting important differences in the data. Total macrophages (F4/80) were significantly higher through all timepoints of the study in IBD vs Control (Figure 21A). In addition, there was a main effect of timepoint in total macrophages for both Control and IBD groups. In the Control group, the total macrophage population was significantly lower than IBD at Day 1 and increased rapidly to a plateau that was maintained from Days 20-240. In contrast, total macrophages in PVAT from IBD mice decreased from Days 1-10 then steadily increased through Day 240 without an apparent plateau (Figure 21A). This suggests that M1 macrophages may be important for healthy aging in mesenteric PVAT.

M2 macrophages (CD206) were initially increased in IBD vs Control during the first 2 timepoints, however at the third timepoint, there started to be a shift between the two groups (Figure 21B). The data at the third timepoint appeared to be growing closer in similarity, with no statistical differences between M2 macrophages in IBD vs Control at Day 10, Day 20, and Day 40. However, on the sixth timepoint (Day 80) the trends went opposite of that of Day 1 and 5. M2 macrophages decreased in IBD vs Control starting at Day 80, with no change at Day 160 and decreased in IBD vs Control at Day 240 once again. We expected control M2 populations to remain steady overtime. Instead, it rose from Days 1-20 until reaching a maintained plateau. In IBD, we expected M2s to steadily decrease over time. Consistent with our hypothesis in IBD, M2s were the highest at Day 1 and Day 5 and decreased to a plateau for the remaining timepoints (Day 40-240).

M1 macrophages (CD68) were significantly higher throughout all time-points (Figure 21C)

in IBD vs Control. A specific trend of interest to point out was the sudden increase M1 macrophages during Day 1 IBD. However, there is a decrease in M1 macrophages in the IBD group in the two timepoints after Day 1, with an upward trend following Day 20. In Control, M1 macrophage numbers remained consistent over time as we predicted. With IBD, we saw and unexpected biphasic response. M1s decreased mostly in two steps between Days 5-10 and 40-80 then remained steady until Day 240.

Overall, our findings suggest that M1 macrophage proliferation is associated with IBD progression. Importantly, M2 macrophage activity in our model was decreased in IBD vs Control, denoting M2s loss of protection during IBD onset.

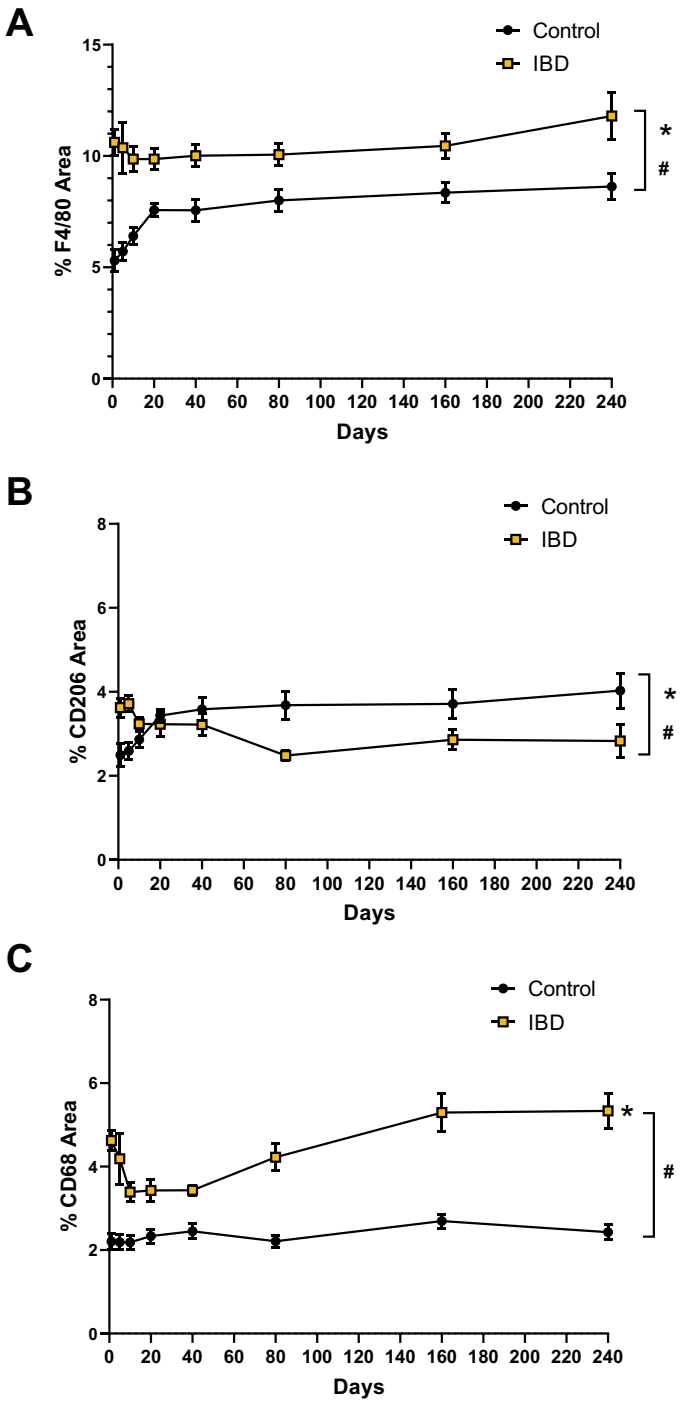

Figure 21. ***Changes in tota1, M2 and M1 macrophage population over time of study.*** Data are mean ± SE percent fluorescent area of total macrophages (A, F4/80), M2-like macrophages (B, CD206) and M1-like macrophages (C, CD68). F4/80 at Days 1-240 in PVAT from Control (black) and IBD (gold) mice. * = $p < 0.05$ for main effect of time and # = $p < 0.05$ for Control vs. IBD via nested two-way ANOVA with Tukey's test.

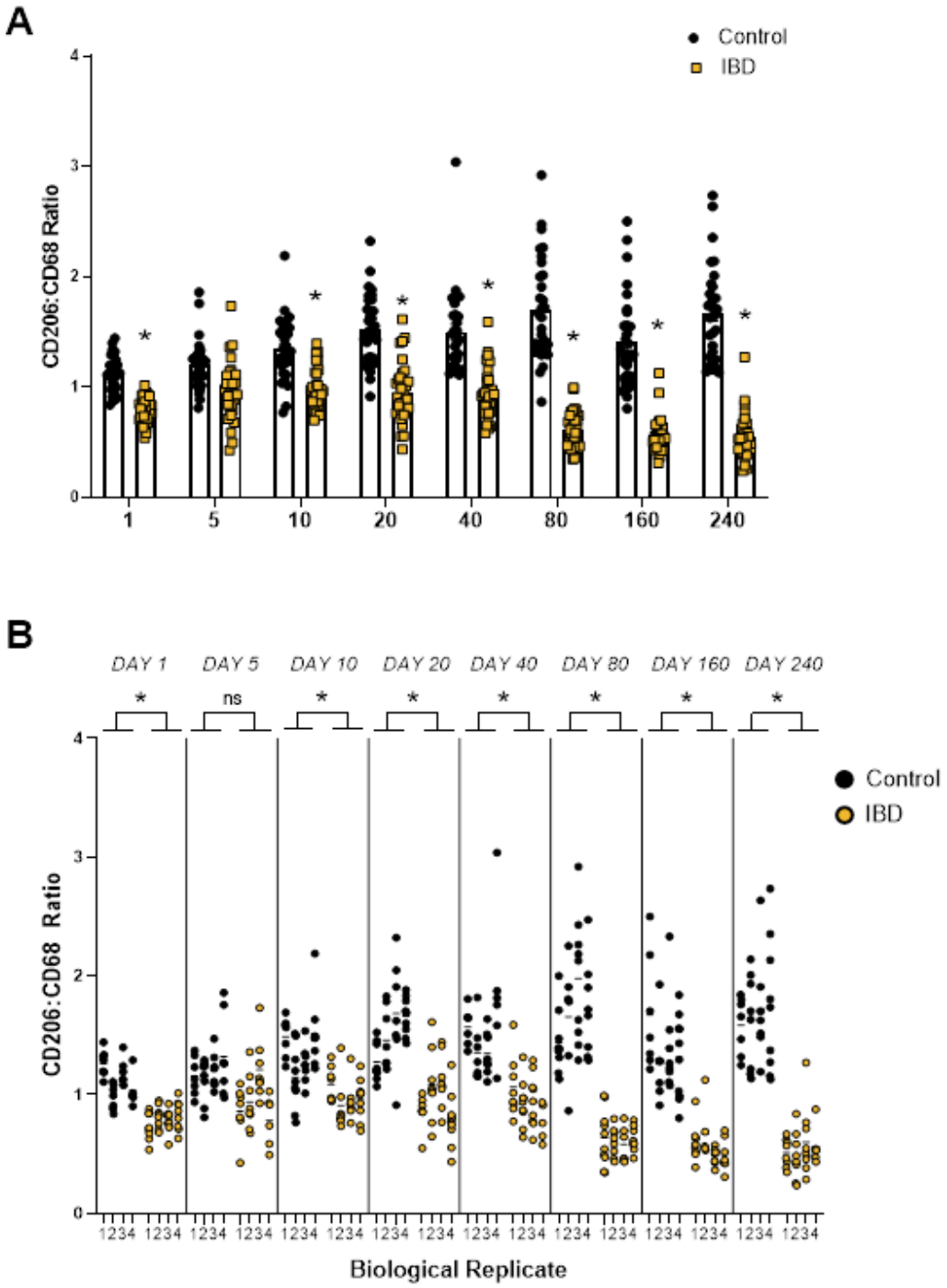

Figure 22. ***Ratio Summary of M2 to M1 macrophages in IBD vs Control.*** A. Overall CD206 (M2):CD68 (M1) ratio. Data are means +/- SE in Control vs IBD PVAT samples labeled for M2-like (CD206+) and M1-like (CD68+) macrophages. B. Summary data from A reflecting images from each biological replicate for F4/80, CD206, and CD68. For all data * = $P < 0.05$ for control vs IBD via nested one-way ANOVA with Sidak test.

M2:M1 ratio throughout IBD progression

To discern the involvement of macrophages and their proliferative subtypes in IBD progression, we showed a ratio summary of CD206 (M2):CD68 (M1). M2:M1 ratio was statistically significant at each of the timepoints in IBD vs Control (Figure 22A). Technical replicates did not affect the trends seen in Figure 22A, per the nested analysis (Figure 22B). Data from Day 1 showed a significant difference of M2:M1 ratio in IBD vs Control (0.78±0.02 vs 1.12±0.03). During Day 5, there is a slight increase in M2:M1 ratio in both IBD and Control group 0.96±0.05 vs 1.19±0.03). Day 10 signified the final increase of M2:M1 ratio in the IBD group, while the Control group continued to increase as IBD progressed. On Day 20, M2:M1 ratio of IBD begins to decrease while Control M2:M1 ratio continues to increase (0.95±0.04 vs 1.52±0.05). Day 40 is characterized by a continued decrease in M2:M1 ratio in the IBD group and a decrease in Control M2:M1 ratio (0.94±0.05 vs 1.49±0.07). Day 80 marks the beginning of the late timepoints. The trends during these timepoints decrease in the IBD group, while the Control group fluctuates. On Day 80, IBD M2:M1 ratio decreases in comparison to Day 40, while Control M2:M1 ratio reaches its peak for the study (0.61±0.02 vs 1.70±0.08). Day 160 features a decrease in IBD M2:M1 ratio and the M2:M1 ratio in the Control group (0.55±0.03 vs 1.4±0.07). Finally, Day 240 features a slight drop and new low for IBD M2:M1 ratio and an increase in Control M2:M1, but not greater than Day 80 Control (0.54±0.03 vs 1.67±0.07).

In IBD, M2:M1 ratio initially increases in the early timepoints; however, after Day 40, there is a significant decrease in the M2:M1 ratio for the remainder of the timepoints (Figure 23). In Control, M2:M1 ratio increased throughout the study, with no plateau and a dip in M2:M1 ratio only during Day 160 (Figure 23). These trends show that a decrease in M2:M1 ratio is associated with progression of IBD. Our data also showed that a ratio-centered view of IBD may be more informative than looking at total macrophages or subtype in isolation. Because both M1 and M2

macrophages have known effects, looking at the ratio rather than each in isolation will better exhibit their collaboration in maintaining homeostasis or their imbalance during disease progression.

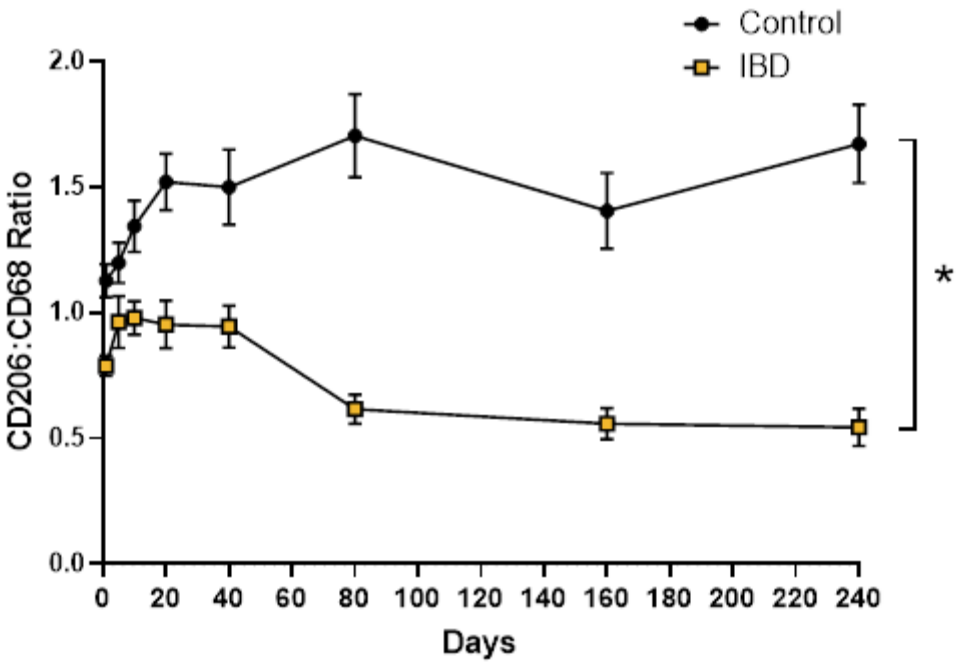

Figure 23. ***Ratio trends over time.*** M2:M1 ratio throughout timepoint study. Data are means +/- SE in Control vs IBD PVAT samples labeled for M2-like (CD206+) and M1-like (CD68+) macrophages. For all data * = $P < 0.05$ for control vs IBD via two-way ANOVA with Tukey's correction. Differences were significant at all timepoints.

Discussion

From our investigations we were able to show that PVAT undergoes multiple changes during IBD progression that likely contribute to the macrophage associated PVAT pro-contractility seen in established disease. PVAT goes through structural and functional changes during IBD progression, resulting in smaller and more densely packed adipocytes and a loss of physiological anti-contractile function for a pro-contractile state. Investigation of macrophage populations showed an increase in total macrophages (F4/80+) in the mesenteric PVAT of IBD vs Control mice. This data is consistent with previous studies showing that depletion of macrophages in IBD mice using clodronate reversed pro-contractile function of PVAT. The studies also took the additional step of measuring M1- (CD68+) and M2-like (CD206+) macrophages throughout the development of IBD. In the timepoint studies, M1-like (CD68) and total (F4/80) macrophages were significantly increased in IBD vs Control at all time-points. M2-like macrophages (CD206) had different trends, with IBD vs Control CD206+ staining being increased at time-points Day 1 and Day 5. From Day 10-40, there was no significant difference in IBD vs Control CD206+ staining. However, the trend would change, with IBD vs Control CD206+ staining significantly decreasing at each timepoint following Day 80 (80, 160, 240). Increased total macrophage presence in IBD within the PVAT depicts the classical response to inflammation. This emphasizes the effect that macrophages have on the underlying blood vessels, especially in the pro-inflammatory associated with IBD. Together with previous functional studies, these data also reinforce the notion that the pro-inflammatory effects associated with IBD it could be resolved by targeting PVAT macrophage accumulation or M1 polarization.

Structural changes to PVAT

Structural changes to PVAT are not specific to only IBD and have clear links to changes in PVAT function. Unfortunately, the majority of studies characterizing PVAT structure look at aortic PVAT, where adipocytes are fundamentally different in origin and size than mesenteric PVAT, making comparisons difficult (Grigoras et al., 2019). Nearly all studies of mesenteric PVAT structure and function are focused on the effects of obesity. Consistent with our observed loss of PVAT anti-contractility in IBD, small arteries of patients with metabolic syndrome or obesity were shown to be compromised in their physiological anti-contractile function. (Aghamohammadzadeh et al., 2013; Greenstein et al., 2009). In our $IL10^{-/-}$ model of IBD, PVAT pro-contractility occurs as PVAT adipocytes decrease in size but increase in density (Figure 3 and 4). Although these changes occur alongside an IBD-associated decrease in body mass, it is critical to note that the total mesenteric PVAT mass is not significantly decreased in our IBD mice at 90 days post gavage (unpublished data). In contrast to IBD, obesity is associated with increased body mass and increased whole-body WAT mass, including PVAT, that occurs via adipocyte hypertrophy and hyperplasia due to chronic surplus in energy intake (Saxton et al., 2019). These changes ultimately induce hypoxia and oxidative stress, which contribute to PVAT dysfunction. In young mice exposed to high fat diet, vascular adipose tissue expansion first occurred via adipocyte hypertrophy, followed by adipocyte hyperplasia after 8 weeks (Wang et al., 2013). While our studies did not measure adipocyte properties over time, the lack of hypertrophy suggests that the hypoxia-related mechanisms may not be as relevant to IBD as they are to obesity. In contrast, increased macrophage content is a common feature of PVAT remodeling in IBD and obesity. Our images of H&E-stained PVAT from IBD mice showed an increase in stromal vascular fraction (Figure 2), and immunostaining confirmed increased macrophage content in PVAT with IBD (Figure 21). In obesity, increased WAT during obesity includes an increase of macrophages. In

PVAT specifically, macrophages increase from 10-15% to 45-50% of the stromal fraction during obesity (Wynn et al., 2013). This increase in macrophages is likely in response to inflammation caused by obesity and its many etiological factors. Understanding the effects of both IBD and obesity are increasingly important. While IBD has historically been associated with decreased body mass, the population of obese IBD patients has expanded to over 20% (Johnson & Loftus, 2020). Given the divergent changes in PVAT structure with obesity and IBD and lack of obese IBD animal models, it is unclear how this comorbidity affects PVAT structure. Functionally, the comorbidity may have vascular consequences similar to those associated with PVAT dysfunction in obesity. Obesity-induced PVAT dysfunction may cause endothelial dysfunction, immune cell infiltration, and migration/proliferation of VSMCs (Stanek et al., 2021). This in turn promotes vascular stiffening and dysfunction, loss of NO bioavailability, and increased inflammation. Based on published studies and our preliminary functional studies, we propose that the macrophage compartment of PVAT represents a promising target that warrants further investigation.

Macrophage polarization in PVAT and IBD

Previous studies in the Boerman laboratory have shown that depletion of macrophages with clodronate reverses PVAT pro-contractility (unpublished data). Macrophage depletion similarly restored sensory nerve-mediated vasodilation in mesenteric arteries that was associated with an increase in gene and protein expression of M1 and M2 macrophage markers (Grunz-Borgmann, 2019). Therefore, we predicted that similar changes may occur in mesenteric PVAT with IBD. To increase the rigor of the study, we measured total, M1-like and M2-like macrophage content in PVAT from 1-240 days of IBD development. Our observation of increased M1 macrophages and decreased M2 macrophages over time with IBD (Figure 21B, 21C) is consistent with many studies of vascular and non-vascular tissues across a wide array of diseases. Similar imbalances in M1-

like vs M2-like macrophages are notably seen in other cardiovascular and inflammatory diseases, including asthma, Type II diabetes, obesity, atherosclerosis, chronic obstructive pulmonary disease, and rheumatoid arthritis. (Fukui et al., 2017; Kraakman et al., 2014; Lyamina & Malyshev, 2014; Saradna et al., 2018).

This is the first study to look at PVAT macrophages over time during IBD development. For both M1 (CD68+) and M2 (CD206+) macrophages in IBD, we predicted that the changes over time would occur steadily with an eventual plateau before Day 240. In the IBD group, M1s actually decreased until day 10, plateaued, then increased again before reaching plateau (Figure 6-20, 21). M2s decreased more steadily but plateaued by Day 80 (Figure 6-20, 21). In the Controls, we expected everything to remain mostly steady across all time points. While M1s stayed at a consistent level (Figure 6-20, 21), M2s rose sharply from Day 1-20 before reaching a plateau (Figure 6-20, 21). This suggests that an increase in M2s over time in healthy mice may be important to preventing PVAT inflammation and pro-contractility. It is difficult to draw comparisons with the literature because few studies have examined PVAT macrophage trends over time in *any* disease state. In a study by Kumar et al., researchers looked at CD163+ (M2-like) macrophages in mesenteric PVAT with obesity and hypertension (Kumar et al., 2021). What they found was that CD163+ macrophages decrease significantly from 10-17 weeks of a high fat diet, but only in females. In our studies, we did not find any sex-related differences, and the timepoints do no incorporate the early changes we see in macrophage populations with IBD. Studies looking at macrophage populations in IBD have focused almost exclusively on the intestine. Here, it is clear that IBD leads to an increase in monocytes, total macrophages and M1 macrophages (Lissner et al., 2015). In a T-cell transfer mouse model of IBD, colonic M1 macrophages increase as early as 12 hours after T-cell transfer and remain elevated for the 3-week duration of studies (Tamoutounour et al., 2012). Similar results were found using a dextran sodium sulfate (DSS)

induced colitis mouse model of IBD (Bain et al., 2013). Our finding that M2 macrophages in PVAT actually decrease in this timeline highlights important differences between the colon and PVAT that warrant further study. The initial increase in M1 and M2 during Day 1 could be due to the start of activation/proliferation of resident and infiltrating monocytes/macrophages. It is possible that the sudden drop and plateau in the following days (Day 5-40) could be due to recruitment of monocytes/macrophages to the intestines, not the PVAT, during this phase of disease development (Figure 21). M1 later increases rapidly while M2 decreases, which may be a result of a delayed proliferative response. Human studies confirm increased colonic M1 macrophages with IBD, but the limitations of human subjects research do not allow for multiple timepoint analysis.

The number and role of M2 macrophages is less studied in IBD. However, there is a general consensus that colonic M2 macrophages oppose inflammation and promote healing, mostly based on numerous studies transferring cultured M2 macrophages into already-inflamed colons (Isidro & Appleyard, 2016). Early studies of M2 macrophages in IBD and other diseases used CD163 as an M2 marker in mice and humans, but more recent work has shown that many unpolarized tissue resident macrophages also express this marker (Kühl et al., 2015). Either way, the CD163 population is increased in the colon of both Crohn's and ulcerative colitis patients (Franzè et al., 2013). The M2 marker CD206 is now more commonly used to identify M2 macrophages in mouse and human studies. In human IBD patients, CD206+ macrophages account for less than a fifth of colonic macrophages, compared to up to 70% for M1s (Vos et al., 2012). In our measurements of PVAT, CD206+ M2s exist in higher numbers, accounting for up to a third of total macrophage fluorescence at early timepoints (Figure 6, 8, 10). Physiologically, the role of M2 macrophages is difficult to pinpoint. Despite the common designation of M2 macrophages as beneficial and anti-inflammatory, the reality is more complex, and there are many studies showing that M2

macrophages can increase alongside M1 macrophages in various disease states. In coronary artery disease, increased M2 macrophages in human coronary artery PVAT are associated with arterial obstruction, calcification and thrombosis (Farias-Itao et al., 2022). Studies using a mouse model of inflammatory arthritis found an increase in M2 macrophages in thoracic PVAT. However, M2s were unchanged in abdominal PVAT, consistent with our findings (Farias-Itao et al., 2022). This study also underscores the important point that thoracic PVAT, often used in mouse studies because of its larger size, is not physiologically equivalent to mesenteric PVAT even in the same disease model.

Comparing specific quantities of macrophage populations between studies can be very difficult because of differences in species, macrophage markers, measurement techniques and disease models. Looking at the M1/M2 or M2/M1 ratio provides an easier way to look at these populations both between and within studies. The M2/M1 ratio in our studies is the clearest example of how macrophage populations diverge over time in IBD vs Control mice (Figure 22-23). These ratios continue to separate, with the Control timepoints never really plateauing and IBD timepoints with decreasing in M2/M1 ratio as time progresses. This suggesting that M2s may play a role in maintaining homeostasis during normal development and aging and that there is a proliferative shift towards a greater M1/M2 ratio in IBD. Increased M1/M2 ratio is associated with other disease and proinflammatory states. This includes ovarian (Zhang et al., 2014) and breast cancer (Oshi et al., 2020), osteoarthritis (Liu et al., 2018), tuberculosis (Yan et al., 2021) and even excess sun-exposure to aged skin (Horiba et al., 2022). This is similar to what is exhibited by our data in Figure 23, which showed a decrease in M2/M1 ratio in IBD vs Control (or an increase in M1/M2 ratio in IBD vs Control). Importantly, in PVAT, increases in M1 and M1/M2 ratio is associated with coronary artery disease (CAD) and progression of atherosclerotic plaques with thrombosis (Farias-Itao et al., 2022). Increased M1/M2 ratio correlated with an increase in arterial

obstruction and lipid content and an increased risk of thrombosis, all important characteristics in CAD. M1 macrophages were associated with a higher risk of coronary thrombosis and were correlated with histological characteristics of atheroma progression and eventual destabilization. M2 macrophages were correlated with calcification, necrotic content, and plaque size, supporting the conclusion that increased M2 macrophages does not always mean a decrease in inflammation of disease signs.

In IBD, the PVAT macrophage ratios have not been fully explored. Recently, a study by Seyedizade et al suggested that targeting the M1 to M2 balance may represent a promising therapeutic target for new IBD treatments (Seyedizade et al., 2020). Particularly, they discussed targeting the imbalance/loss of M2 macrophage function by regulating factors that are involved in macrophage proliferation. Our data suggest that such treatments may also be helpful for the cardiovascular consequences of IBD. In Figure 23, we were able to show that IBD progression was associated with an imbalance (in comparison to Control) of M2/M1 ratio, with a decrease in both M2 population (Figure 21) and a decrease in M2 to M1 ratio in IBD vs Control. In reference to the Seyedizade paper, intervention directed towards restoration of M2 macrophage imbalances could be a possible therapeutic target for IBD.

Physiological relevance of selected timepoints

The timepoints for this study were chosen carefully to include times before during after typical IBD diagnosis age in most human patients. In a study done in Olsted County, MN, the median age of ulcerative colitis and Crohn's disease diagnosis was 34.9 years and 29.5 years, respectively (Aniwan, Harmsen, et al., 2018). Most people worldwide are diagnosed between ages 15 and 35. According to study conducted by Dutta & Sengupta, the correlation between human and mice ages can be calculated out to 1 human year = 9 mouse days (Dutta & Sengupta, 2016).

This is important to consider when conducting medical research utilizing a mouse model. This would mean that the range of our study would show mice between human age 3 (Day 1) to about age 30 (Day 240). The time-point study depicts the changes in macrophage proliferation during normal age range of IBD diagnosis.

In the interpretation of all timepoint data, it is important to consider the level of colon inflammation present in conjunction with changes in PVAT macrophage populations. While colons were collected and fixed for all mice at each timepoint, COVID-related staff changes and delays at core facilities have delayed inflammation scoring past the time of thesis submission. However, previous studies have characterized intestinal inflammation in the IL-$10^{-/-}$ IBD model over several disease timepoints. In two studies, little to no colon inflammation was observed through 6 weeks (42 days) of age. Inflammation significantly increased by 10 weeks (70 days), with a further increase by 16 weeks (112 days) (Gomes-Santos et al., 2012; Hale & Greer, 2012). A third study found that histological colitis began in some mice by 2 weeks (14 days) but then progressed as described in other studies through 16 weeks (Kullberg et al., 1998). Thus, it is likely that any changes occurring in PVAT macrophages before Day 20 and possibly up to Day 40, occur before disease can be identified histologically in the colon. Total and M1 macrophages actually decrease in the IBD mice until about Day 20, then both start to rise (Figure 21). In the same period, M2s increase in the Control but not IBD mice (Figure 21). The changes we see are consistent with histological onset of significant histological disease. If we clinically intervened early with treatments to increase M2s, decrease M1s or both, perhaps we could prevent both the macrophage population changes and possibly even prevent some the associated colon inflammation. Even if it didn't improve colon inflammation, our previous studies linking macrophages to vascular dysfunction suggest that such treatments could restore normal vasodilation and blood flow to mesenteric arteries.

What is the source of PVAT macrophages in IBD?

The source of PVAT macrophages during the inflammatory response associated with IBD, namely monocyte and macrophages, remains unclear and must be discussed. There are two general possibilities for where these monocytes are coming from: initiation and proliferation by resident immune cells already present in the tissue or infiltration by circulating immune cells that are responding to inflammatory signaling factors (Wynn et al., 2013). Resident macrophages are present in most of the tissue in the body and have distinct subsets depending on the needs of their tissue microenvironment. They are the first to "react" to an inflammatory response, proliferate and release signaling factors to recruit more immune cells. These macrophages may then be polarized into M1 or M2 phenotypes based on local inflammatory mediators. After prolonged inflammation, there is buildup of cellular debris and death of resident macrophages. These macrophages must then be replaced by circulating monocytes that are continuously responding to the signaling factors released by the remaining resident macrophages. Because all timepoints in the Control group showed significant M1 and M2 macrophage populations in PVAT, it is safe to say that resident macrophages are present in the PVAT (Figure 6-21). Circulating monocytes can have differing roles. Classical ly6c^{hi} monocytes patrol the extravascular space while Ly6c^{lo} nonclassical monocytes patrol the vasculature. Each of these subtypes differentiation from Ly6C^{high} progenitors, however non-classical monocytes differentiate in a process dependent on transcription factor Nr4a1(Wynn et al., 2013). Classical monocytes respond to inflammation and are recruited to the site where they will differentiate into macrophages. Non-classical monocytes utilize the integrin lymphocyte function-associated antigen 1 (LFA-1) to patrol the vasculature itself, allowing them to move against the flow of blood if necessary. They have a key role in clearing damaged endothelial cells, which maintains the integrity of the vasculature. And while each phenotype has vital roles, classical monocytes comprise around 80-95% of the circulating monocytes while non-

classical monocytes make up around 2-11% of them. (Sampath et al., 2018). Regardless of subtype, movement of circulating monocytes from the blood into the vessel wall and PVAT, represents the "inside-out" model of inflammation. Following monocyte chemotactic recruitment, monocytes differentiate, and activation based on the microenvironment and are retained, amplifying inflammation (Shirai et al., 2015).

More recently, vascular studies had noted the occurrence of "outside-in" vascular inflammation, where inflammation starts in the adventitia and/or PVAT and progresses inward. This mechanism has been proposed in studies of atherosclerosis (Herrmann et al., 2001), hypertension (Trott & Harrison, 2014), and aneurysm (Gavrila et al., 2005) although most studies do not address PVAT specifically. The majority of studies focus on atherosclerosis and show that after vessel injury, the adventitia and PVAT become populated with macrophages and other immune cells before the development of intimal plaques. The mechanism of recruitment is not clear, but upregulation of monocyte chemoattractant protein 1 (MCP-1) is a key factor (Maiellaro & Taylor, 2007). Studies in our lab support the participation of this mechanism, as mesenteric arteries express increased MCP-1 in IBD vs control mice. Expression levels in PVAT have not yet been defined, but tissue collection for RNA sequencing of PVAT is in progress.

With respect to our investigations, we predict that both resident and circulating macrophages contribute to the chronic inflammation observed in IBD. Initial activation of resident macrophages could be the key factor causing the large M1-like and total macrophage increase detected during Day 1 and Day 5 of the time-point study (Figure 6 and 8). Critically, after Day 5, M1-like staining decreases dramatically (Figure 10-21). This could indicate an attempt by the immune system to resolve inflammation. However, it is also possible that the drop in M1-like macrophages is due to macrophage cell death in response to the chronic inflammation and bacterial translocation that occurred with gavage treatment of *H. hepaticus.* Further, it is important to

consider that existing unpolarized and M2 macrophages can re-polarize into M1-like macrophages based on the local environmental stimuli.

PVAT and creeping fat with IBD

Creeping fat is hyperplasia of the mesenteric fat immediately adjacent to the inflamed segments of the intestines. Although creeping fat is well established as a hallmark of Crohn's disease in humans, the cause of the phenomenon is unclear. There have been connections made between bacterial translocation and the development of creeping fat (Kredel & Siegmund, 2014). This does occur in normal, healthy gut physiology; however, it is strongly increased during Crohn's. This could allude to chronic bacterial translocation leading to the adipose tissue hyperplasia in creeping fat of Crohn's disease. It is unclear whether direct parallels can be drawn between intestinal creeping fat and inflamed PVAT with IBD, largely because creeping fat is not currently a feature in any mouse models of IBD, and human studies have yet to thoroughly investigate PVAT features. Structurally, there appears to be similarities, as creeping fat contains small, hyperplastic adipocytes similar to our observations in mesenteric PVAT (Figure 2-4) (Kredel & Siegmund, 2014). Creeping fat is a potent producer of cytokines, growth factors, adipokines and fatty acids, much like the pro-inflammatory shift seen in PVAT across various diseases (Karaskova et al., 2021). Macrophages are also present in creeping fat, once again alluding to the profound effect that the macrophages could be eliciting on the surround fat tissue, much like in inflammatory PVAT. However, creeping fat has a macrophage population different than both colonic macrophages in IBD and our observations in PVAT. Creeping fat has increased M1 and M2 macrophages (Karaskova et al., 2021), with a proportionally greater expansion of the M2 population (Kredel et al., 2013). Interestingly, the investigations by Kredel et al. discovered that creeping fat adipose favored M2-like macrophages that, of course, release anti-inflammatory

cytokines (Kredel et al., 2013). If creeping fat is housing M2-like macrophages, then this provides evidence that creeping fat may be an attempt by the body to resolve inflammation or at the very least, deter it. Additional studies looking at both PVAT and creeping fat are needed to determine whether their pathogenic changes have truly common features and/or timelines in IBD.

Predicted effects of PVAT macrophage population changes on vascular function

From our preliminary clodronate studies, we know that depleting macrophages after 90 days makes PVAT neutral, meaning that the PVAT is no longer pro- or anti-contractile. In reference to the Day 80 timepoint (Figure 16), our data shows that M1s are increased and M2s are decreased. This correlates with the partial rescue effects observed during the clodronate studies. Clodronate depletes global macrophage levels, including M1 and M2 subtypes. Intervention with Clodronate at Day 90 of IBD progression would decrease M1 levels, which would decrease the pro-constrictive effects that they elicit. However, it would also exhaust the already depleted M2 macrophages, not allowing the full-saving effect necessary for the vessel to become anticontractile once again.

Study limitations

It must be noted that there were limitations to our study. Firstly, we used one antibody marker each for total, M1-like and M2-like macrophage staining. These markers, F4/80, CD68 and CD206, are expressed on the surface of all, M1-like, and M2-like macrophages, respectively. However, CD206 and CD68 these are not specific to only macrophages. CD68 highly expressed by cells of the mononuclear phagocyte lineage, including dendritic cells (Chistiakov et al., 2017). It is expressed in considerably lower levels by lymphoid cells such as B lymphocytes and T lymphocytes. CD206 is also not solely expressed in macrophages and has been shown to be

expressed on dendritic and endothelial cells as well (Azad et al., 2014). Despite these limiting factors, each of these markers are widely accepted and used as markers of their respective macrophage populations in mice.

Compounding to the limitations of only using one marker for each of the antibodies of interest, we were also limited on our ability to count the exact cell number of macrophages per FOV like we have done previously in the mesenteric artery adventitia. This is due to numerous factors. First, the PVAT is much larger in volume than the adventitia and contains a great deal more macrophages. Second, and more important to this study, the complexity of the macrophage cell shape and their ability to squeeze between adipocytes makes them difficult to count accurately. Future studies can address most of these limitations by (1) using flow cytometry to characterize macrophage populations with multiple markers and (2) using single cell RNA sequencing of dissociated PVAT to define the genotypes of all PVAT cell types. However, we believe that the immunofluorescent measurements in intact PVAT were the critical first step as they measured cell populations in the intact tissue without the enzymatic perturbations needed to isolate single cells for flow cytometry or RNA sequencing.

Another limitation is within our animal model itself. While our model is sufficient for studying IBD, it more closely resembles the pathophysiology of Crohn's disease than Ulcerative colitis because it includes small intestine and rectal inflammation. However, it should also be mentioned that our mouse model is unable to replicate the cobble-stone appearance of lesions that occurs in the colons of human Crohn's patients. The implications of IL-10 knockout must also be taken into consideration. Kim et al. postulated that IL-10 induction by M2 macrophages gives functional characteristics that help resolve inflammation through reduction of pro-inflammatory pathways and secreting factors (Kim et al., 2020). Another group, da Silva et al., showed that IL-10 cytokine release was necessary for M2 macrophages anti-inflammatory effects in a model of

inflammatory muscle pain (da Silva et al., 2015). This is relevant to our study because, one could argue, that our model cannot respond in a true anti-inflammatory fashion because our model lacks the IL-10 necessary for physiological M2 induction. It is possible that our M2 macrophages may not work in the same anti-inflammatory sense as seen *in vitro* or in human patients but could be a less functional phenotypic subtype of the M2-like proliferation. This could point to what is occurring in Figure 22c, with M2-like macrophages being less pronounced after the first initial time-points even while total macrophages were increased. Lack of IL-10 in our genetically deficient models may cause a less pronounced M2 macrophage proliferation in response to the increased M1-like proliferation shown in Figure 22b. And while disruption in the equilibrium of M1 vs M2 is associated with IBD, our model may not accurately depict the exact M2-like macrophages involvement in IBD because of lack of IL-10. To control for this possibility, studies could be repeated in a different mouse model, such as the T-cell transfer or dextran sulfate sodium models, to see if our results can be recapitulated. These other models also have key differences compared to human IBD patients, but replication of mouse studies in multiple models for any IBD study would increase the rigor and impact of the results.

Overall, the experiments from this thesis found evidence of a structural and functional changes occurring in PVAT that coincide with an imbalance in macrophage proliferation during IBD pathogenesis. Under physiological conditions, PVAT is anti-contractile in vascular function. In our foundational studies, we were able to exhibit loss of this anti-contractile function into a pro-contractile state during IBD progression. To go along with these functional changes, we were also able to determine that PVAT goes through structural changes as well. We were able to show that under IBD progression, PVAT undergoes structural changes, with decreased size and increased density vs Control PVAT. Importantly, macrophages are also found within the PVAT and vasculature, and play a role in maintenance of vascular homeostasis and function. They are able to

proliferate into subtypes with alternate functions in response to physiological changes occurring in the vasculature. In our foundational studies, we were able to determine that IBD progression was associated with an increase of macrophages in the mesenteric vascular wall in IBD vs Control. To further explore the involvement of macrophage proliferation in IBD development, we performed a timepoint study focused on the changes that occur in total, M1 and M2 macrophages in PVAT. We found that IBD progression was associated with an increase in total and M1 and a decrease in M2 macrophages in IBD vs Control. IBD was also associated with a decrease in M2:M1 macrophage ratio compared to Control. Importantly, the trends of the M2:M1 ratio continued to separate as IBD progressed, alluding to the importance of M2 macrophages in vascular homeostasis. These results are consistent with other studies in PVAT, IBD and other diseases associated with imbalances in macrophage proliferation. Although additional studies are needed to provide a more complete understanding of PVAT and macrophages in the progression of IBD, the current data suggest that PVAT macrophages represent a promising target to improve vascular function and therefore intestinal blood flow in IBD.

References

Abram, C. L., & Lowell, C. A. (2009). The ins and outs of leukocyte integrin signaling. *Annu Rev Immunol*, *27*, 339-362. https://doi.org/10.1146/annurev.immunol.021908.132554

Aghamohammadzadeh, R., Greenstein, A. S., Yadav, R., Jeziorska, M., Hama, S., Soltani, F., Pemberton, P. W., Ammori, B., Malik, R. A., Soran, H., & Heagerty, A. M. (2013). Effects of bariatric surgery on human small artery function: evidence for reduction in perivascular adipocyte inflammation, and the restoration of normal anticontractile activity despite persistent obesity. *J Am Coll Cardiol*, *62*(2), 128-135. https://doi.org/10.1016/j.jacc.2013.04.027

Akil, L., & Ahmad, H. A. (2011). Relationships between obesity and cardiovascular diseases in four southern states and Colorado. *J Health Care Poor Underserved*, *22*(4 Suppl), 61-72. https://doi.org/10.1353/hpu.2011.0166

Aniwan, S., Harmsen, W. S., Tremaine, W. J., Kane, S. V., & Loftus, E. V., Jr. (2018). Overall and Cause-Specific Mortality of Inflammatory Bowel Disease in Olmsted County, Minnesota, From 1970 Through 2016. *Mayo Clin Proc*, *93*(10), 1415-1422. https://doi.org/10.1016/j.mayocp.2018.03.004

Aniwan, S., Pardi, D. S., Tremaine, W. J., & Loftus, E. V., Jr. (2018). Increased Risk of Acute Myocardial Infarction and Heart Failure in Patients With Inflammatory Bowel Diseases. *Clin Gastroenterol Hepatol*, *16*(10), 1607-1615.e1601. https://doi.org/10.1016/j.cgh.2018.04.031

Arango Duque, G., & Descoteaux, A. (2014). Macrophage cytokines: involvement in immunity and infectious diseases. *Front Immunol*, *5*, 491. https://doi.org/10.3389/fimmu.2014.00491

Azad, A. K., Rajaram, M. V., & Schlesinger, L. S. (2014). Exploitation of the Macrophage Mannose Receptor (CD206) in Infectious Disease Diagnostics and Therapeutics. *J Cytol Mol Biol*, *1*(1). https://doi.org/10.13188/2325-4653.1000003

Bain, C. C., & Mowat, A. M. (2014). Macrophages in intestinal homeostasis and inflammation. *Immunol Rev*, *260*(1), 102-117. https://doi.org/10.1111/imr.12192

Bain, C. C., Scott, C. L., Uronen-Hansson, H., Gudjonsson, S., Jansson, O., Grip, O., Guilliams, M., Malissen, B., Agace, W. W., & Mowat, A. M. (2013). Resident and pro-inflammatory macrophages in the colon represent alternative context-dependent fates of the same Ly6Chi monocyte precursors. *Mucosal Immunol*, *6*(3), 498-510. https://doi.org/10.1038/mi.2012.89

Barrett, T. J. (2020). Macrophages in Atherosclerosis Regression. *Arterioscler Thromb Vasc Biol*, *40*(1), 20-33. https://doi.org/10.1161/atvbaha.119.312802

Bergheanu, S. C., Bodde, M. C., & Jukema, J. W. (2017). Pathophysiology and treatment of atherosclerosis : Current view and future perspective on lipoprotein modification treatment. *Neth Heart J*, *25*(4), 231-242. https://doi.org/10.1007/s12471-017-0959-2

Bi, Y., Chen, J., Hu, F., Liu, J., Li, M., & Zhao, L. (2019). M2 Macrophages as a Potential Target for Antiatherosclerosis Treatment. *Neural Plast*, *2019*, 6724903. https://doi.org/10.1155/2019/6724903

Bilski, J., Mazur-Bialy, A., Wojcik, D., Surmiak, M., Magierowski, M., Sliwowski, Z., Pajdo, R., Kwiecien, S., Danielak, A., Ptak-Belowska, A., & Brzozowski, T. (2019). Role of Obesity, Mesenteric Adipose Tissue, and Adipokines in Inflammatory Bowel Diseases. *Biomolecules*, *9*(12). https://doi.org/10.3390/biom9120780

Brown, N. K., Zhou, Z., Zhang, J., Zeng, R., Wu, J., Eitzman, D. T., Chen, Y. E., & Chang, L. (2014). Perivascular adipose tissue in vascular function and disease: a review of current research and animal models. *Arterioscler Thromb Vasc Biol*, *34*(8), 1621-1630. https://doi.org/10.1161/atvbaha.114.303029

Bussey, C. E., Withers, S. B., Aldous, R. G., Edwards, G., & Heagerty, A. M. (2016). Obesity-Related Perivascular Adipose Tissue Damage Is Reversed by Sustained Weight Loss in the Rat. *Arterioscler Thromb Vasc Biol*, *36*(7), 1377-1385. https://doi.org/10.1161/atvbaha.116.307210

Cannon, B., & Nedergaard, J. (2004). Brown adipose tissue: function and physiological significance. *Physiol Rev*, *84*(1), 277-359. https://doi.org/10.1152/physrev.00015.2003

Castoldi, A., Naffah de Souza, C., Câmara, N. O., & Moraes-Vieira, P. M. (2015). The Macrophage Switch in Obesity Development. *Front Immunol*, *6*, 637. https://doi.org/10.3389/fimmu.2015.00637

Chang, L., Garcia-Barrio, M. T., & Chen, Y. E. (2020). Perivascular Adipose Tissue Regulates Vascular Function by Targeting Vascular Smooth Muscle Cells. *Arterioscler Thromb Vasc Biol*, *40*(5), 1094-1109. https://doi.org/10.1161/atvbaha.120.312464

Chatterjee, T. K., Stoll, L. L., Denning, G. M., Harrelson, A., Blomkalns, A. L., Idelman, G., Rothenberg, F. G., Neltner, B., Romig-Martin, S. A., Dickson, E. W., Rudich, S., & Weintraub, N. L. (2009). Proinflammatory phenotype of perivascular adipocytes: influence of high-fat feeding. *Circ Res*, *104*(4), 541-549. https://doi.org/10.1161/circresaha.108.182998

Cheng, C. K., Bakar, H. A., Gollasch, M., & Huang, Y. (2018). Perivascular Adipose Tissue: the Sixth Man of the Cardiovascular System. *Cardiovasc Drugs Ther*, *32*(5), 481-502. https://doi.org/10.1007/s10557-018-6820-z

Chistiakov, D. A., Killingsworth, M. C., Myasoedova, V. A., Orekhov, A. N., & Bobryshev, Y. V. (2017). CD68/macrosialin: not just a histochemical marker. *Laboratory Investigation*, *97*(1), 4-13. https://doi.org/10.1038/labinvest.2016.116

Crohn, B. B., GINZBURG, L., & OPPENHEIMER, G. D. (1932). REGIONAL ILEITIS: A PATHOLOGIC AND CLINICAL ENTITY. *Journal of the American Medical Association*, *99*(16), 1323-1329. https://doi.org/10.1001/jama.1932.02740680019005

Csige, I., Ujvárosy, D., Szabó, Z., Lőrincz, I., Paragh, G., Harangi, M., & Somodi, S. (2018). The Impact of Obesity on the Cardiovascular System. *J Diabetes Res*, *2018*, 3407306. https://doi.org/10.1155/2018/3407306

da Silva, M. D., Bobinski, F., Sato, K. L., Kolker, S. J., Sluka, K. A., & Santos, A. R. (2015). IL-10 cytokine released from M2 macrophages is crucial for analgesic and anti-inflammatory effects of acupuncture in a model of inflammatory muscle pain. *Mol Neurobiol*, *51*(1), 19-31. https://doi.org/10.1007/s12035-014-8790-x

Davies, L. C., Jenkins, S. J., Allen, J. E., & Taylor, P. R. (2013). Tissue-resident macrophages. *Nat Immunol*, *14*(10), 986-995. https://doi.org/10.1038/ni.2705

de Gaetano, M., Crean, D., Barry, M., & Belton, O. (2016). M1- and M2-Type Macrophage Responses Are Predictive of Adverse Outcomes in Human Atherosclerosis. *Front Immunol*, *7*, 275. https://doi.org/10.3389/fimmu.2016.00275

Dutta, S., & Sengupta, P. (2016). Men and mice: Relating their ages. *Life Sciences*, *152*, 244-248. https://doi.org/https://doi.org/10.1016/j.lfs.2015.10.025

Ensan, S., Li, A., Besla, R., Degousee, N., Cosme, J., Roufaiel, M., Shikatani, E. A., El-Maklizi, M., Williams, J. W., Robins, L., Li, C., Lewis, B., Yun, T. J., Lee, J. S., Wieghofer, P., Khattar, R., Farrokhi, K., Byrne, J., Ouzounian, M., . . . Robbins, C. S. (2016). Self-renewing resident arterial macrophages arise from embryonic CX3CR1(+) precursors and circulating monocytes immediately after birth. *Nat Immunol*, *17*(2), 159-168. https://doi.org/10.1038/ni.3343

Epelman, S., Lavine, K. J., & Randolph, G. J. (2014). Origin and functions of tissue macrophages. *Immunity*, *41*(1), 21-35. https://doi.org/10.1016/j.immuni.2014.06.013

Farias-Itao, D. S., Pasqualucci, C. A., Andrade, R. A. d., Silva, L. F. F. d., Yahagi-Estevam, M., Lage, S. H. G., Leite, R. E. P., Campo, A. B., & Suemoto, C. K. (2022). Macrophage Polarization in the Perivascular Fat Was Associated With Coronary Atherosclerosis. *Journal of the American Heart Association*, *11*(6), e023274. https://doi.org/doi:10.1161/JAHA.121.023274

Feng, Q., Xu, X. T., Zhou, Y., Yan, Y. Q., Ran, Z. H., & Zhu, J. (2018). Creeping fat in patients with ileo-colonic Crohn's disease correlates with disease activity and severity of inflammation: A preliminary study using energy spectral computed tomography. *J Dig Dis*, *19*(8), 475-484. https://doi.org/10.1111/1751-2980.12652

Franzè, E., Caruso, R., Stolfi, C., Sarra, M., Cupi, M. L., Caprioli, F., Monteleone, I., Zorzi, F., De Nitto, D., Colantoni, A., Biancone, L., Pallone, F., & Monteleone, G. (2013). Lesional Accumulation of CD163-Expressing Cells in the Gut of Patients with Inflammatory Bowel Disease. *PLOS ONE*, *8*(7), e69839. https://doi.org/10.1371/journal.pone.0069839

Fukui, S., Iwamoto, N., Takatani, A., Igawa, T., Shimizu, T., Umeda, M., Nishino, A., Horai, Y., Hirai, Y., Koga, T., Kawashiri, S. Y., Tamai, M., Ichinose, K., Nakamura, H., Origuchi, T., Masuyama, R., Kosai, K., Yanagihara, K., & Kawakami, A. (2017). M1 and M2 Monocytes in Rheumatoid Arthritis: A Contribution of Imbalance of M1/M2 Monocytes to Osteoclastogenesis. *Front Immunol*, *8*, 1958. https://doi.org/10.3389/fimmu.2017.01958

Gabanyi, I., Muller, P. A., Feighery, L., Oliveira, T. Y., Costa-Pinto, F. A., & Mucida, D. (2016). Neuro-immune Interactions Drive Tissue Programming in Intestinal Macrophages. *Cell*, *164*(3), 378-391. https://doi.org/10.1016/j.cell.2015.12.023

Gavrila, D., Li, W. G., McCormick, M. L., Thomas, M., Daugherty, A., Cassis, L. A., Miller, F. J., Oberley, L. W., Dellsperger, K. C., & Weintraub, N. L. (2005). Vitamin E Inhibits Abdominal Aortic Aneurysm Formation in Angiotensin II–Infused Apolipoprotein E–Deficient Mice. *Arteriosclerosis, Thrombosis, and Vascular Biology*, *25*(8), 1671-1677. https://doi.org/doi:10.1161/01.ATV.0000172631.50972.0f

Gomes-Santos, A. C., Moreira, T. G., Castro-Junior, A. B., Horta, B. C., Lemos, L., Cruz, D. N., Guimarães, M. A., Cara, D. C., McCafferty, D. M., & Faria, A. M. (2012). New insights into the immunological changes in IL-10-deficient mice during the course of spontaneous inflammation in the gut mucosa. *Clin Dev Immunol*, *2012*, 560817. https://doi.org/10.1155/2012/560817

Gravina, A. G., Dallio, M., Masarone, M., Rosato, V., Aglitti, A., Persico, M., Loguercio, C., & Federico, A. (2018). Vascular Endothelial Dysfunction in Inflammatory Bowel Diseases: Pharmacological and Nonpharmacological Targets. *Oxid Med Cell Longev*, *2018*, 2568569. https://doi.org/10.1155/2018/2568569

Greenstein, A. S., Khavandi, K., Withers, S. B., Sonoyama, K., Clancy, O., Jeziorska, M., Laing, I., Yates, A. P., Pemberton, P. W., Malik, R. A., & Heagerty, A. M. (2009). Local inflammation and hypoxia abolish the protective anticontractile properties of perivascular fat in obese patients. *Circulation*, *119*(12), 1661-1670. https://doi.org/10.1161/circulationaha.108.821181

Grigoras, A., Amalinei, C., Balan, R. A., Giusca, S. E., & Caruntu, I. D. (2019). Perivascular adipose tissue in cardiovascular diseases-an update. *Anatol J Cardiol*, *22*(5), 219-231. https://doi.org/10.14744/AnatolJCardiol.2019.91380

Grunz-Borgmann, E. A. (2019). Macrophage Depletion Reverses Impaired Sympathetic Vasoconstriction and Sensory Vasodilation of Mesenteric Arteries from IL-10-/- Mice with Inflammatory Bowel Disease. *FASEB J 33*.

Grunz-Borgmann, E. L., Jones, B. W., & Boerman, E. M. (2019). Macrophage Depletion Reverses Impaired Sympathetic Vasoconstriction and Sensory Vasodilation of Mesenteric Arteries from IL-10−/− Mice with Inflammatory Bowel Disease. *The FASEB Journal*, *33*(S1), 523.528-523.528. https://doi.org/https://doi.org/10.1096/fasebj.2019.33.1_supplement.523.8

Guan, Q. (2019). A Comprehensive Review and Update on the Pathogenesis of Inflammatory Bowel Disease. *J Immunol Res*, *2019*, 7247238. https://doi.org/10.1155/2019/7247238

Guzik, T. J., Skiba, D. S., Touyz, R. M., & Harrison, D. G. (2017). The role of infiltrating immune cells in dysfunctional adipose tissue. *Cardiovasc Res*, *113*(9), 1009-1023. https://doi.org/10.1093/cvr/cvx108

Hale, L. P., & Greer, P. K. (2012). A novel murine model of inflammatory bowel disease and inflammation-associated colon cancer with ulcerative colitis-like features. *PLOS ONE*, *7*(7), e41797. https://doi.org/10.1371/journal.pone.0041797

Han, X., Ding, S., Jiang, H., & Liu, G. (2021). Roles of Macrophages in the Development and Treatment of Gut Inflammation [Review]. *Frontiers in Cell and Developmental Biology*, *9*. https://doi.org/10.3389/fcell.2021.625423

Harris, N. R., Carter, P. R., Lee, S., Watts, M. N., Zhang, S., & Grisham, M. B. (2010). Association between blood flow and inflammatory state in a T-cell transfer model of inflammatory bowel disease in mice. *Inflamm Bowel Dis*, *16*(5), 776-782. https://doi.org/10.1002/ibd.21126

Herrmann, J., Lerman, L. O., Rodriguez-Porcel, M., Holmes, D. R., Jr., Richardson, D. M., Ritman, E. L., & Lerman, A. (2001). Coronary vasa vasorum neovascularization precedes epicardial

endothelial dysfunction in experimental hypercholesterolemia. *Cardiovasc Res*, *51*(4), 762-766. https://doi.org/10.1016/s0008-6363(01)00347-9

Honda, M., Surewaard, B. G. J., Watanabe, M., Hedrick, C. C., Lee, W. Y., Brown, K., McCoy, K. D., & Kubes, P. (2020). Perivascular localization of macrophages in the intestinal mucosa is regulated by Nr4a1 and the microbiome. *Nat Commun*, *11*(1), 1329. https://doi.org/10.1038/s41467-020-15068-4

Horiba, S., Kami, R., Tsutsui, T., & Hosoi, J. (2022). IL-34 Downregulation–Associated M1/M2 Macrophage Imbalance Is Related to Inflammaging in Sun-Exposed Human Skin. *JID Innov*, *2*(3), 100112. https://doi.org/10.1016/j.xjidi.2022.100112

Hultén, L., Lindhagen, J., Lundgren, O., Fasth, S., & Ahrén, C. (1977). Regional intestinal blood flow in ulcerative colitis and Crohn's disease. *Gastroenterology*, *72*(3), 388-396.

Isidro, R. A., & Appleyard, C. B. (2016). Colonic macrophage polarization in homeostasis, inflammation, and cancer. *Am J Physiol Gastrointest Liver Physiol*, *311*(1), G59-73. https://doi.org/10.1152/ajpgi.00123.2016

Johnson, A. M., & Loftus, E. V. (2020). Impact of Obesity on the Management of Inflammatory Bowel Disease. *Gastroenterol Hepatol (N Y)*, *16*(7), 350-359.

Karaskova, E., Velganova-Veghova, M., Geryk, M., Foltenova, H., Kucerova, V., & Karasek, D. (2021). Role of Adipose Tissue in Inflammatory Bowel Disease. *Int J Mol Sci*, *22*(8). https://doi.org/10.3390/ijms22084226

Ketonen, J., Shi, J., Martonen, E., & Mervaala, E. (2010). Periadventitial adipose tissue promotes endothelial dysfunction via oxidative stress in diet-induced obese C57Bl/6 mice. *Circ J*, *74*(7), 1479-1487. https://doi.org/10.1253/circj.cj-09-0661

Kim, Y. K., Kim, S. E., Chang Park, H., Hwang, J. H., & Lee, H. T. (2020). Human recombinant IL-10 reduces xenogenic cytotoxicity via macrophage M2 polarization. *Biochem Biophys Rep*, *24*, 100857. https://doi.org/10.1016/j.bbrep.2020.100857

Kraakman, M. J., Murphy, A. J., Jandeleit-Dahm, K., & Kammoun, H. L. (2014). Macrophage Polarization in Obesity and Type 2 Diabetes: Weighing Down Our Understanding of Macrophage Function? [Mini Review]. *Frontiers in Immunology*, *5*. https://doi.org/10.3389/fimmu.2014.00470

Kredel, L. I., Batra, A., Stroh, T., Kühl, A. A., Zeitz, M., Erben, U., & Siegmund, B. (2013). Adipokines from local fat cells shape the macrophage compartment of the creeping fat in Crohn's disease. *Gut*, *62*(6), 852-862. https://doi.org/10.1136/gutjnl-2011-301424

Kredel, L. I., & Siegmund, B. (2014). Adipose-Tissue and Intestinal Inflammation – Visceral Obesity and Creeping Fat [Review]. *Frontiers in Immunology*, *5*. https://doi.org/10.3389/fimmu.2014.00462

Kühl, A. A., Erben, U., Kredel, L. I., & Siegmund, B. (2015). Diversity of Intestinal Macrophages in Inflammatory Bowel Diseases. *Front Immunol*, *6*, 613. https://doi.org/10.3389/fimmu.2015.00613

Kullberg, M. C., Ward, J. M., Gorelick, P. L., Caspar, P., Hieny, S., Cheever, A., Jankovic, D., & Sher, A. (1998). Helicobacter hepaticus triggers colitis in specific-pathogen-free interleukin-10 (IL-10)-deficient mice through an IL-12- and gamma interferon-dependent mechanism. *Infect Immun*, *66*(11), 5157-5166. https://doi.org/10.1128/iai.66.11.5157-5166.1998

Leitner, B. P., Huang, S., Brychta, R. J., Duckworth, C. J., Baskin, A. S., McGehee, S., Tal, I., Dieckmann, W., Gupta, G., Kolodny, G. M., Pacak, K., Herscovitch, P., Cypess, A. M., & Chen, K. Y. (2017). Mapping of human brown adipose tissue in lean and obese young men. *Proceedings of the National Academy of Sciences*, *114*(32), 8649-8654. https://doi.org/doi:10.1073/pnas.1705287114

Lissner, D., Schumann, M., Batra, A., Kredel, L. I., Kühl, A. A., Erben, U., May, C., Schulzke, J. D., & Siegmund, B. (2015). Monocyte and M1 Macrophage-induced Barrier Defect Contributes to Chronic Intestinal Inflammation in IBD. *Inflamm Bowel Dis*, *21*(6), 1297-1305. https://doi.org/10.1097/mib.0000000000000384

Liu, B., Zhang, M., Zhao, J., Zheng, M., & Yang, H. (2018). Imbalance of M1/M2 macrophages is linked to severity level of knee osteoarthritis. *Exp Ther Med*, *16*(6), 5009-5014. https://doi.org/10.3892/etm.2018.6852

Lyamina, S., & Malyshev, I. (2014). Imbalance of immune response functional phenotype and alveolar macrophages phenotype in COPD. *European Respiratory Journal*, *44*(Suppl 58), P1483.

Maiellaro, K., & Taylor, W. R. (2007). The role of the adventitia in vascular inflammation. *Cardiovasc Res*, *75*(4), 640-648. https://doi.org/10.1016/j.cardiores.2007.06.023

Mills, C. D., Kincaid, K., Alt, J. M., Heilman, M. J., & Hill, A. M. (2000). M-1/M-2 macrophages and the Th1/Th2 paradigm. *J Immunol*, *164*(12), 6166-6173. https://doi.org/10.4049/jimmunol.164.12.6166

Moore, K. J., Sheedy, F. J., & Fisher, E. A. (2013). Macrophages in atherosclerosis: a dynamic balance. *Nat Rev Immunol*, *13*(10), 709-721. https://doi.org/10.1038/nri3520

Mulya, A., & Kirwan, J. P. (2016). Brown and Beige Adipose Tissue: Therapy for Obesity and Its Comorbidities? *Endocrinol Metab Clin North Am*, *45*(3), 605-621. https://doi.org/10.1016/j.ecl.2016.04.010

Murray, P. J. (2017). Macrophage Polarization. *Annual Review of Physiology*, *79*(1), 541-566. https://doi.org/10.1146/annurev-physiol-022516-034339

Na, Y. R., Stakenborg, M., Seok, S. H., & Matteoli, G. (2019). Macrophages in intestinal inflammation and resolution: a potential therapeutic target in IBD. *Nature Reviews Gastroenterology & Hepatology*, *16*(9), 531-543. https://doi.org/10.1038/s41575-019-0172-4

Norton, C. E., Grunz-Borgmann, E. A., Hart, M. L., Jones, B. W., Franklin, C. L., & Boerman, E. M. (2021). Role of perivascular nerve and sensory neurotransmitter dysfunction in inflammatory bowel disease. *Am J Physiol Heart Circ Physiol*, *320*(5), H1887-h1902. https://doi.org/10.1152/ajpheart.00037.2021

Nosalski, R., & Guzik, T. J. (2017). Perivascular adipose tissue inflammation in vascular disease. *Br J Pharmacol*, *174*(20), 3496-3513. https://doi.org/10.1111/bph.13705

Okamoto, E., Couse, T., De Leon, H., Vinten-Johansen, J., Goodman, R. B., Scott, N. A., & Wilcox, J. N. (2001). Perivascular inflammation after balloon angioplasty of porcine coronary arteries. *Circulation*, *104*(18), 2228-2235. https://doi.org/10.1161/hc4301.097195

Orecchioni, M., Ghosheh, Y., Pramod, A. B., & Ley, K. (2019). Macrophage Polarization: Different Gene Signatures in M1(LPS+) vs. Classically and M2(LPS-) vs. Alternatively Activated Macrophages. *Front Immunol*, *10*, 1084. https://doi.org/10.3389/fimmu.2019.01084

Oshi, M., Tokumaru, Y., Asaoka, M., Yan, L., Satyananda, V., Matsuyama, R., Matsuhashi, N., Futamura, M., Ishikawa, T., Yoshida, K., Endo, I., & Takabe, K. (2020). M1 Macrophage and M1/M2 ratio defined by transcriptomic signatures resemble only part of their conventional clinical characteristics in breast cancer. *Sci Rep*, *10*(1), 16554. https://doi.org/10.1038/s41598-020-73624-w

Park, S. H. (2021). Regulation of Macrophage Activation and Differentiation in Atherosclerosis. *J Lipid Atheroscler*, *10*(3), 251-267. https://doi.org/10.12997/jla.2021.10.3.251

Qi, X.-Y., Qu, S.-L., Xiong, W.-H., Rom, O., Chang, L., & Jiang, Z.-S. (2018). Perivascular adipose tissue (PVAT) in atherosclerosis: a double-edged sword. *Cardiovascular Diabetology*, *17*(1), 134. https://doi.org/10.1186/s12933-018-0777-x

Richard, A. J., White, U., Elks, C. M., & Stephens, J. M. (2000). Adipose Tissue: Physiology to Metabolic Dysfunction. In K. R. Feingold, B. Anawalt, A. Boyce, G. Chrousos, W. W. de Herder, K. Dhatariya, K. Dungan, J. M. Hershman, J. Hofland, S. Kalra, G. Kaltsas, C. Koch, P. Kopp, M. Korbonits, C. S. Kovacs, W. Kuohung, B. Laferrère, M. Levy, E. A. McGee, R. McLachlan, J. E. Morley, M. New, J. Purnell, R. Sahay, F. Singer, M. A. Sperling, C. A. Stratakis, D. L. Trence, & D. P. Wilson (Eds.), *Endotext*. MDText.com, Inc.

Röszer, T. (2018). Understanding the Biology of Self-Renewing Macrophages. *Cells*, *7*(8). https://doi.org/10.3390/cells7080103

Sakers, A., De Siqueira, M. K., Seale, P., & Villanueva, C. J. (2022). Adipose-tissue plasticity in health and disease. *Cell*, *185*(3), 419-446. https://doi.org/10.1016/j.cell.2021.12.016

Sampath, P., Moideen, K., Ranganathan, U. D., & Bethunaickan, R. (2018). Monocyte Subsets: Phenotypes and Function in Tuberculosis Infection [Mini Review]. *Frontiers in Immunology*, *9*. https://doi.org/10.3389/fimmu.2018.01726

Saradna, A., Do, D. C., Kumar, S., Fu, Q. L., & Gao, P. (2018). Macrophage polarization and allergic asthma. *Transl Res*, *191*, 1-14. https://doi.org/10.1016/j.trsl.2017.09.002

Saxton, S. N., Clark, B. J., Withers, S. B., Eringa, E. C., & Heagerty, A. M. (2019). Mechanistic Links Between Obesity, Diabetes, and Blood Pressure: Role of Perivascular Adipose Tissue. *Physiol Rev*, *99*(4), 1701-1763. https://doi.org/10.1152/physrev.00034.2018

Scientific, T. F. (2021). *Macrophage Cell Overview*. Retrieved July 30 from https://www.thermofisher.com/us/en/home/life-science/cell-analysis/cell-analysis-learning-center/immunology-at-work/macrophage-cell-overview.html#references

Seyedizade, S. S., Afshari, K., Bayat, S., Rahmani, F., Momtaz, S., Rezaei, N., & Abdolghaffari, A. H. (2020). Current Status of M1 and M2 Macrophages Pathway as Drug Targets for Inflammatory Bowel Disease. *Arch Immunol Ther Exp (Warsz)*, *68*(2), 10. https://doi.org/10.1007/s00005-020-00576-4

Shapouri-Moghaddam, A., Mohammadian, S., Vazini, H., Taghadosi, M., Esmaeili, S.-A., Mardani, F., Seifi, B., Mohammadi, A., Afshari, J. T., & Sahebkar, A. (2018). Macrophage plasticity, polarization, and function in health and disease. *Journal of Cellular Physiology*, *233*(9), 6425-6440. https://doi.org/https://doi.org/10.1002/jcp.26429

Shirai, T., Hilhorst, M., Harrison, D. G., Goronzy, J. J., & Weyand, C. M. (2015). Macrophages in vascular inflammation--From atherosclerosis to vasculitis. *Autoimmunity*, *48*(3), 139-151. https://doi.org/10.3109/08916934.2015.1027815

Siegel-Axel, D. I., & Häring, H. U. (2016). Perivascular adipose tissue: An unique fat compartment relevant for the cardiometabolic syndrome. *Rev Endocr Metab Disord*, *17*(1), 51-60. https://doi.org/10.1007/s11154-016-9346-3

Skiba, D. S., Nosalski, R., Mikolajczyk, T. P., Siedlinski, M., Rios, F. J., Montezano, A. C., Jawien, J., Olszanecki, R., Korbut, R., Czesnikiewicz-Guzik, M., Touyz, R. M., & Guzik, T. J. (2017). Anti-atherosclerotic effect of the angiotensin 1-7 mimetic AVE0991 is mediated by inhibition of perivascular and plaque inflammation in early atherosclerosis. *Br J Pharmacol*, *174*(22), 4055-4069. https://doi.org/10.1111/bph.13685

Soltis, E. E., & Cassis, L. A. (1991). Influence of perivascular adipose tissue on rat aortic smooth muscle responsiveness. *Clin Exp Hypertens A*, *13*(2), 277-296. https://doi.org/10.3109/10641969109042063

Stanek, A., Brożyna-Tkaczyk, K., & Myśliński, W. (2021). The Role of Obesity-Induced Perivascular Adipose Tissue (PVAT) Dysfunction in Vascular Homeostasis. *Nutrients*, *13*(11). https://doi.org/10.3390/nu13113843

Stenmark, K. R., Yeager, M. E., El Kasmi, K. C., Nozik-Grayck, E., Gerasimovskaya, E. V., Li, M., Riddle, S. R., & Frid, M. G. (2013). The adventitia: essential regulator of vascular wall structure and function. *Annu Rev Physiol*, *75*, 23-47. https://doi.org/10.1146/annurev-physiol-030212-183802

Szasz, T., Bomfim, G. F., & Webb, R. C. (2013). The influence of perivascular adipose tissue on vascular homeostasis. *Vasc Health Risk Manag*, *9*, 105-116. https://doi.org/10.2147/vhrm.S33760

Szasz, T., & Webb, R. C. (2012). Perivascular adipose tissue: more than just structural support. *Clin Sci (Lond)*, *122*(1), 1-12. https://doi.org/10.1042/cs20110151

Tamoutounour, S., Henri, S., Lelouard, H., de Bovis, B., de Haar, C., van der Woude, C. J., Woltman, A. M., Reyal, Y., Bonnet, D., Sichien, D., Bain, C. C., Mowat, A. M., Reis e Sousa, C., Poulin, L. F., Malissen, B., & Guilliams, M. (2012). CD64 distinguishes macrophages from dendritic cells

in the gut and reveals the Th1-inducing role of mesenteric lymph node macrophages during colitis. *European Journal of Immunology*, *42*(12), 3150-3166. https://doi.org/https://doi.org/10.1002/eji.201242847

Thornton, M., & Solomon, M. J. (2002). Crohn's disease: in defense of a microvascular aetiology. *Int J Colorectal Dis*, *17*(5), 287-297. https://doi.org/10.1007/s00384-002-0408-5

Trayhurn, P., & Beattie, J. H. (2001). Physiological role of adipose tissue: white adipose tissue as an endocrine and secretory organ. *Proc Nutr Soc*, *60*(3), 329-339. https://doi.org/10.1079/pns200194

Trott, D. W., & Harrison, D. G. (2014). The immune system in hypertension. *Adv Physiol Educ*, *38*(1), 20-24. https://doi.org/10.1152/advan.00063.2013

Virdis, A., Duranti, E., Rossi, C., Dell'Agnello, U., Santini, E., Anselmino, M., Chiarugi, M., Taddei, S., & Solini, A. (2015). Tumour necrosis factor-alpha participates on the endothelin-1/nitric oxide imbalance in small arteries from obese patients: role of perivascular adipose tissue. *Eur Heart J*, *36*(13), 784-794. https://doi.org/10.1093/eurheartj/ehu072

Vos, A. C., Wildenberg, M. E., Arijs, I., Duijvestein, M., Verhaar, A. P., de Hertogh, G., Vermeire, S., Rutgeerts, P., van den Brink, G. R., & Hommes, D. W. (2012). Regulatory macrophages induced by infliximab are involved in healing *in vivo* and *in vitro*. *Inflamm Bowel Dis*, *18*(3), 401-408. https://doi.org/10.1002/ibd.21818

Wang, Q. A., Tao, C., Gupta, R. K., & Scherer, P. E. (2013). Tracking adipogenesis during white adipose tissue development, expansion and regeneration. *Nat Med*, *19*(10), 1338-1344. https://doi.org/10.1038/nm.3324

Weisberg, S. P., McCann, D., Desai, M., Rosenbaum, M., Leibel, R. L., & Ferrante, A. W., Jr. (2003). Obesity is associated with macrophage accumulation in adipose tissue. *J Clin Invest*, *112*(12), 1796-1808. https://doi.org/10.1172/jci19246

Westcott, E. B., & Segal, S. S. (2013). Perivascular innervation: a multiplicity of roles in vasomotor control and myoendothelial signaling. *Microcirculation*, *20*(3), 217-238. https://doi.org/10.1111/micc.12035

Wu, H., Hu, T., Zhang, L., Xia, X., Liu, X., Zhu, Q., Wang, M., Sun, Z., Hao, H., Cui, Y., Parrish, A. R., Li, D. P., Hill, M. A., Xu, C., & Liu, Z. (2022). Abdominal Aortic Endothelial Dysfunction Occurs in Female Mice With Dextran Sodium Sulfate-Induced Chronic Colitis Independently of Reactive Oxygen Species Formation. *Front Cardiovasc Med*, *9*, 871335. https://doi.org/10.3389/fcvm.2022.871335

Wynn, T. A., Chawla, A., & Pollard, J. W. (2013). Macrophage biology in development, homeostasis and disease. *Nature*, *496*(7446), 445-455. https://doi.org/10.1038/nature12034

Xia, N., Horke, S., Habermeier, A., Closs, E. I., Reifenberg, G., Gericke, A., Mikhed, Y., Münzel, T., Daiber, A., Förstermann, U., & Li, H. (2016). Uncoupling of Endothelial Nitric Oxide Synthase in Perivascular Adipose Tissue of Diet-Induced Obese Mice. *Arterioscler Thromb Vasc Biol*, *36*(1), 78-85. https://doi.org/10.1161/atvbaha.115.306263

Xia, N., & Li, H. (2017). The role of perivascular adipose tissue in obesity-induced vascular dysfunction. *Br J Pharmacol*, *174*(20), 3425-3442. https://doi.org/10.1111/bph.13650

Xiong, W., Zhao, X., Villacorta, L., Rom, O., Garcia-Barrio, M. T., Guo, Y., Fan, Y., Zhu, T., Zhang, J., Zeng, R., Chen, Y. E., Jiang, Z., & Chang, L. (2018). Brown Adipocyte-Specific PPARγ (Peroxisome Proliferator-Activated Receptor γ) Deletion Impairs Perivascular Adipose Tissue Development and Enhances Atherosclerosis in Mice. *Arterioscler Thromb Vasc Biol*, *38*(8), 1738-1747. https://doi.org/10.1161/atvbaha.118.311367

Xue, J., Schmidt, S. V., Sander, J., Draffehn, A., Krebs, W., Quester, I., De Nardo, D., Gohel, T. D., Emde, M., Schmidleithner, L., Ganesan, H., Nino-Castro, A., Mallmann, M. R., Labzin, L., Theis, H., Kraut, M., Beyer, M., Latz, E., Freeman, T. C., . . . Schultze, J. L. (2014). Transcriptome-based network analysis reveals a spectrum model of human macrophage activation. *Immunity*, *40*(2), 274-288. https://doi.org/10.1016/j.immuni.2014.01.006

Yan, C., Wang, M., Sun, F., Cao, L., Jia, B., & Xia, Y. (2021). Macrophage M1/M2 ratio as a predictor of pleural thickening in patients with tuberculous pleurisy. *Infectious Diseases Now*, *51*(7), 590-595. https://doi.org/https://doi.org/10.1016/j.idnow.2020.11.013

Zatterale, F., Longo, M., Naderi, J., Raciti, G. A., Desiderio, A., Miele, C., & Beguinot, F. (2019). Chronic Adipose Tissue Inflammation Linking Obesity to Insulin Resistance and Type 2 Diabetes. *Front Physiol*, *10*, 1607. https://doi.org/10.3389/fphys.2019.01607

Zhang, C., Yang, M., & Ericsson, A. C. (2021). Function of Macrophages in Disease: Current Understanding on Molecular Mechanisms. *Front Immunol*, *12*, 620510. https://doi.org/10.3389/fimmu.2021.620510

Zhang, M., He, Y., Sun, X., Li, Q., Wang, W., Zhao, A., & Di, W. (2014). A high M1/M2 ratio of tumor-associated macrophages is associated with extended survival in ovarian cancer patients. *J Ovarian Res*, *7*, 19. https://doi.org/10.1186/1757-2215-7-19

Zhang, Y., Proenca, R., Maffei, M., Barone, M., Leopold, L., & Friedman, J. M. (1994). Positional cloning of the mouse obese gene and its human homologue. *Nature*, *372*(6505), 425-432. https://doi.org/10.1038/372425a0